Pure hydrogen from biogas: intensified methane dry reforming in a two-zone fluidized bed reactor using permselective membranes

P. Durán, A. Sanz-Martínez, J. Soler, M. Menéndez, J. Herguido

PII: S1385-8947(19)30673-4
DOI: https://doi.org/10.1016/j.cej.2019.03.199
Reference: CEJ 21323

To appear in: *Chemical Engineering Journal*

Received Date: 4 January 2019
Revised Date: 21 March 2019
Accepted Date: 22 March 2019

Please cite this article as: P. Durán, A. Sanz-Martínez, J. Soler, M. Menéndez, J. Herguido, Pure hydrogen from biogas: intensified methane dry reforming in a two-zone fluidized bed reactor using permselective membranes, *Chemical Engineering Journal* (2019), doi: https://doi.org/10.1016/j.cej.2019.03.199

Pure hydrogen from biogas: intensified methane dry reforming in a two-zone fluidized bed reactor using permselective membranes

P. Durán, A. Sanz-Martínez, J. Soler, M. Menéndez, J. Herguido*

Catalysis, Molecular Separations and Reactor Engineering Group (CREG), Aragon Institute of Engineering Research (I3A). Department of Chemical and Environmental Engineering. University of Zaragoza, Spain

jhergui@unizar.es

Abstract:

Methane dry reforming of biogas can be a sustainable source of hydrogen but the development of this technology is hindered by limitations such as endothermicity and catalyst deactivation by coke. A two zone fluidized bed reactor coupling permselective Pd/Ag membranes counteracts them and allows to intensify the process obtaining a stable pure hydrogen production. Here we report the effect of operation variables (i.e., temperature, total bed height, nature and partial pressure of regenerative agent, relative height of the regeneration and reaction zones, and use of an activation period) on the yield to hydrogen and stability of the process. Hydrogen over-yields, compared with the conventional fluidized bed reactor, in the range of +200% to +100% were obtained for the entire interval of temperatures 475-575°C whilst maintaining stable operation by continuous catalyst regeneration. Around 70% of it was pure hydrogen coming from the permeate side of the membranes. The proposed reactor configuration greatly increases both methane conversion and selectivity to hydrogen (expressed as H_2/CO ratio), not only in relation to our own conventional reactor findings but also regarding other published results.

Keywords:

Biogas; methane dry reforming; hydrogen; membranes; fluidized bed; process intensification.

INTRODUCTION

The production of hydrogen from biogas by methane dry reforming (MDR) could be an environmentally-friendly application for this renewable resource [1]. Biogas is usually generated by the anaerobic decomposition of organic wastes (i.e., biomass, municipal solids, and industrial or livestock residues), and it is composed mainly of methane and carbon dioxide as well as other gases, such as carbon monoxide, hydrogen, nitrogen, oxygen, ammonia, hydrogen sulfide and siloxanes, that are present in minor proportions [2, 3]. Taking apart these contaminants, that must be removed prior to almost any further treatment, MDR seems to be an interesting process for the biogas since the CH_4/CO_2 mix can be transformed to produce H_2 and CO, according to the reaction (r.1). Moreover, and unlike the traditional process of steam reforming of methane (SRM) (r.2), MDR avoids the energy requirements associated with steam production. Hence, MDR arises as a good approach to the use of biogas as a non-fossil, clean, and renewable source to obtain pure hydrogen that could be used as a fuel, for example, for automotive applications. In this case, an unavoidable task will be the subsequent purification of the produced hydrogen in order to make it suitable for a proton-exchange membrane fuel cell (PEMFC). In fact, a CO content lower than a few tens of ppm [4] is required to avoid the poisoning of the platinum-alloy catalyst used in PEMFC anodes. Additionally, an important drawback of the MDR of biogas as a source of pure hydrogen is that, at low pressures, reverse water gas shift reaction (r.3) would consume the target hydrogen to produce carbon monoxide and water [5]. An ideal solution would consist of removing hydrogen from the reaction atmosphere as soon as it is produced.

$CH_4 + CO_2 \leftrightarrows 2CO + 2H_2$ $\quad \Delta H^0_{298} = 247$ kJ/mol (r.1)

$CH_4 + H_2O \leftrightarrows CO + 3H_2$ $\quad \Delta H^0_{298} = 206$ kJ/mol (r.2)

$CO + H_2O \leftrightarrows CO_2 + H_2$ $\quad \Delta H^0_{298} = -41$ kJ/mol (r.3)

$CH_4 \leftrightarrows C_{(s)} + 2H_2$ $\quad \Delta H^0_{298} = 75$ kJ/mol (r.4)

$2CO \leftrightarrows C_{(s)} + CO_2$ $\quad \Delta H^0_{298} = -173$ kJ/mol (r.5)

A way to deal with both aforementioned requirements for produced hydrogen (i.e., purification and removal from the reaction medium) would be the incorporation of permselective Pd/Ag membranes

(MB) in the reactor. This kind of membrane allows to obtain as permeate a pure hydrogen stream suitable to be used, for our example, in low temperature fuel cells for automotive applications. Pd based membranes have been widely employed in packed bed membrane reactors for steam reforming of methane [6-11] and a few authors have studied fluidized bed membrane reactors for hydrogen production by water gas shift [12], Even simultaneous CO_2 capture with pure hydrogen production could be possible in a system combining a fluidized bed membrane reactor with chemical looping [13, 14]. Unfortunately, the removal of hydrogen results in an atmosphere of reaction in which the rate of catalyst deactivation by coke deposition is increased. Indeed, under these circumstances methane decomposition (r.4) and *Boudouard* equilibrium (r.5) appear as the main reactions leading to coke deposition on the catalyst surface. The relationship between catalyst deactivation and coke formation is described in a recent kinetic study [15].

Furthermore MDR presents some other constraints in relation to SRM, due mainly to the absence of water in the feeding stream, such as: (*i*) its high endothermicity, (*ii*) the lower amount of hydrogen produced by mol of methane reformed, and (*iii*) the higher tendency to coke formation.

To cope with all these disadvantages (*i* to *iii*), a two-zone fluidized bed reactor (TZFBR) has been proposed to carry out the MDR, allowing in this way the simultaneous catalyst regeneration in a single unit. In the non-conventional TZFBR reacting system [16, 17], due to its design, both processes can be carried out simultaneously: the catalytic dry reforming reaction in the upper zone of the bed, and the regeneration of the catalyst in the lower zone. The formation of two zones is achieved by feeding the biogas stream at an intermediate height point of the fluidized bed and an oxidizing stream at the bottom of the fluidized bed. The combination of TZFBR with the above-mentioned Pd/Ag membranes (MB) is an outstanding case of process integration by providing in one single device (*i*) catalytic MDR reaction, (*ii*) catalyst regeneration by coke combustion, and (*iii*) separation of the produced hydrogen. The TZFBR+MB configuration, thanks to the simultaneous regeneration, may provide a steady state operation in conditions where a conventional fluidized bed membrane reactor would usually suffer deactivation by coking (e.g., , [18, 19]).

TZFBR+MB configuration has been tested in our laboratory [20-23]. Different processes of catalytic alkane dehydrogenation have been tested in TZFBR+MB reactors using several types of membrane, such as palladium membranes over ceramic hollow fiber or commercial membranes over a porous metallic support. Recently, the viability and stability of this process configuration has been analyzed for methane dry reforming [24]. It has been found that a TZFBR+MB system provides a much greater methane conversion than its counterpart without membranes, while offering the added advantage of operating in a steady mode. The feasibility of using CO_2 as regenerating gas was also observed, with effectiveness similar to O_2. Moreover, several catalysts were tested and Ni-Ce/Al_2O_3 was chosen as the best one because it had the slowest coke formation. The high conversions of methane and yields to hydrogen achieved, the capacity to reach steady state operation counteracting coke deactivation, and the high purity of the hydrogen obtained permeating through the membrane, are clear reasons to state the high potential of TZFBR+MB for DRM. Nevertheless, a more in-depth study and further analysis on the effect of the different operational variables was considered necessary in order to improve the production of hydrogen. To that end, a further experimental analysis has been carried out, which forms the basis of this work.

So, the objective of this work is to analyze the effect of operation variables such as temperature, nature of regenerative agent, or ratio between the height of the regeneration and reaction zones, among others, for a detailed improvement of the DRM process in a TZFBR+MB system. In this regard, two important aspects will be considered in the enhancement of the innovative intensified process: (*i*) its stability over time-on-stream and (*ii*) its gain in hydrogen yield over a conventional fluidized bed reactor (FBR).

Complementarily to the improvement of performance carried out through this work, a techno-economic study for the MDR in a TZFBR+MB has been published elsewhere [25]. The production costs of high purity hydrogen are estimated for the TZFBR+MB system, as well as for hydrogen produced from its integration with a Steam Iron Process (SIP). In this last case, SIP acts as an additional hydrogen separation step for the gas coming out from the TZFBR+MB retentate.

EXPERIMENTAL

The reaction system, whose detailed scheme has been already shown elsewhere [24], is based in a quartz-made cylindrical reactor 2.8 cm in internal diameter and 30 cm in height. The arrangement of its different elements and streams is shown in Figure 1a.

The oxidant stream is fed through the bottom of a porous quartz plate (with 90 μm pore size), which acts both as gas distributor and as catalytic bed support inside the reactor. The biogas stream is fed through a quartz tube (external diameter 4 mm) at an intermediate height point in the fluidized bed, z_0 centimeters above the distributor plate. The lower end of this upper distributor constitutes a T-shaped tube with two orifice distributors symmetrically located with respect to the reactor axis. A synthetic biogas composed of equimolar mixtures of CH_4 and CO_2 was used in this work, simulating a previously desulfurized biogas [26]. Each reactive gas flowrate is controlled by a set of mass flow controllers (*Alicat Scientific*). The reactor is placed inside an electrical oven. An immersed thermocouple connected to a PID control (Controller 3116, *Eurotherm*) measures the temperature. The reactor exit stream is condensed in an ice-salt-ethanol bath to remove water, and the remaining gases are analyzed on-line by gas chromatography (Varian CP3800). The GC is equipped with a molecular sieve (*MolSieve 13X*) to analyze permanent gases (H_2, CO, N_2, CH_4 and O_2) and a micropacked column (*HayeSep® Q*) to detect CO_2.

Two different Pd/Ag membranes supported on porous stainless steel were connected in parallel and incorporated inside the reactor (sketched by red lines in Figure 1a). Each commercial membrane (*REB Research®*) used in this work has a total length of 15.2 cm, an external diameter of 0.32 cm, and a thickness of the Pd/Ag layer of 76 μm. Both membranes are sealed at their lower end and joined by their upper end and brazed to a stainless steel stub connected to an external vacuum pump (2P-3 - *Telstar*). When the reactor is operated in a TZFBR+MB configuration, the pump provides a low pressure in the permeate side (c.a. 6 mbar). The stream coming from this side is also analyzed online by gas chromatography, working alternatively with the retentate stream by switching a 3-way valve.

A Ni(5 %)- Ce(10 %)/Al_2O_3 catalyst was selected (all percentages in mass), among those used in the previous study [24], for this work. Nickel (5 %) provided a good catalytic activity to MDR and the addition

of cerium (10 %) improved oxygen exchange and minimized coke formation. We synthesized the catalyst by an incipient wetness method with a double step of metal impregnation (firstly with Ni and then with Ce). The Al_2O_3 support (*Sasol*, *Puralox®* SCCa-150/200) with a particle diameter of 106-180 μm was calcined at 950°C for 1h. Then it was impregnated with a solution (86.5 mL, 0.98M) of nickel nitrate $Ni(NO_3)_2.6H_2O$ (*Sigma Aldrich*, 99.999 %), dried at 120°C for 24h, and calcined at 950°C for 1h. Finally, we repeated these last steps with a solution (77.3 mL, 0.92M) of cerium nitrate $Ce(NO_3)_2.6H_2O$ (*Sigma Aldrich*, 99.999$_{wt}$%). The specific surface area (BET method), chemical composition (XRF), and structural analysis of crystalline species (XRD) were measured for samples of the catalyst both before and after reaction.

We carried out two different types of experiments, depending on the reactor configuration:

(*i*) *conventional fluidized bed reactor (FBR)* with co-feeding of synthetic biogas into the bottom of the bed, and maintaining inactive both the upper distributor (i.e., without feeding any gas stream through it) and the membrane line (i.e., without applying vacuum or suction in the permeate side, and thus without hydrogen permeation). These experiments correspond to those carried out according to the schemes labeled as b in Figure 1 (b1 and b2).

(ii) *two zone fluidized bed reactor with membranes (TZFBR+MB)* with separate feeding of synthetic biogas (through the upper distributor) and oxidants (through the bottom of the bed) and extracting hydrogen through the membrane by operating the vacuum pump. These experiments correspond to those carried out according to the sketches labeled as c in Figure 1 (c1 to c3).

The catalyst load was always 30 g, and different weights of Al_2O_3 with the same particle diameter (106-180 μm) were used as an inert solid in the bed. A heating rate of 2°C/min was used to reach the reaction temperature as a way to minimize the damage of membranes by thermal stress. MDR was then carried out at different reaction temperatures between 475°C and 575°C under the operation conditions detailed in Table 1. The gas flowrate was also modified in these experiments: the relative gas velocity (u_r) whit respect to the minimum fluidizing velocity (u_{mf} = 9.1 $cm^3(STP)/(cm^2.min)$) was set in u_r = 3 for the reaction zone of the bed, and in u_r = 1.2 for the regeneration one. Regarding the composition of the gas, a 60% by volume of the total feed was synthetic biogas (CH_4:CO_2 = 1), 5% was N_2 (in order to be

used as internal tracer), a variable percentage was oxidant agent, and the rest was Ar to complete the balance. Typically, experiments started operating the setup as a conventional fluidized bed reactor (FBR) for 2 hours and then the configuration was changed to a TZFBR+MB one (i.e., we fed synthetic biogas and regenerating gas through their respective inlet points and we turned on hydrogen extraction through the membranes).

After each experiment, we regenerated the catalyst bed at 525°C using a stream at u_r = 1.2 containing 10% oxygen in Ar, and we measured by gas chromatography the amount of carbon oxides formed (CO and CO_2), in order to evaluate the total amount of coke accumulated on both catalyst surface and membranes surface along the reaction test. Then, and previously to another run, we temporally removed the membranes from the reactor and reactivated the catalytic bed at 700°C using a stream at u_r = 2.0 containing 50% hydrogen in Ar.

RESULTS

Prior to the reaction tests, we characterized the performance of membranes by measuring their permeation flux at different temperatures and hydrogen pressures. The characterization was carried out with the membranes inside the reactor but without catalytic bed. A constant flow rate of H_2 was supplied at the bottom inlet of the reactor together with a variable flow rate of Ar. The permeate outflow was quantified and analyzed, finding that no Ar was flowing through the membranes, illustrating their high selectivity towards hydrogen permeation. Figure 2 shows an example of this characterization, from experiments working with 80 mL(STP)·min^{-1} as inlet flowrate of hydrogen and two different temperatures, 500 and 550°C. As it can be seen, there is not a remarkable difference in hydrogen permeation with the temperature. Moreover, H_2 permeation trend against the square root of the pressure drop (*Sieverts*' driving force) is not linear for high values of this driving force; surely this is due to the scarcity of hydrogen in the retentate when a large fraction of the fed hydrogen has permeated through the membrane.

Reference results

A first series of MDR tests was carried out trying to replicate the previously reported results [24]. To this end, we adopted the configuration b1 from Figure 1 in the fluidized bed reactor working with a total height of the catalytic bed of h_0 = 15 cm and the rest of operating conditions those of the Table 1. After two hours operating in FBR mode, we switched the distribution of feeding gas streams using multiple-way valves to adopt the TZFBR+MB configuration depicted as c1 in Figure 1.

Figure 3a shows the flows of hydrogen obtained over time-on-stream for both FBR and TZFBR+MB bed configurations. When we co-fed the biogas through the bottom of the bed the hydrogen flow clearly decreased with time due to the effect of coking. The total flow of hydrogen produced when membranes were working (by turning on the vacuum pump) and biogas was fed to a height z_0 = 2 cm into the bed, clearly overperforms the former one. Feeding 10% of oxygen through the bottom of the bed, in this new configuration, helped to achieve a more stable behavior of the system. However, a slight drop of hydrogen flow can still be perceived. Unlike in previous work [24], we quantified the two different streams of hydrogen obtained from the TZFBR+MB reactor (i.e., pure hydrogen obtained as permeate stream through the membrane, $H_{2(p)}$, and hydrogen mixed with other gases in the retentate stream, $H_{2(r)}$). At standard operating conditions used for the experiment of Figure 3a, the pure $H_{2(p)}$ stream represented around 85% of the total hydrogen production, and clearly surpassed the flow rate of non-pure hydrogen obtained in the conventional FBR configuration. The flow rate of hydrogen produced in FBR configuration (roughly 1.6 mmol.min^{-1}, corresponding to a fractional conversion of $x_{CH4} = x_{CO2}$ = 0.254), represented a partial pressure of hydrogen in the outlet stream p_{H2}= 132 mbar, and then a *Sieverts*'s driving force of 9 mbar$^{0.5}$. Therefore, according to Figure 2 it implies a hydrogen flux of 2.2 mL(STP).min^{-1}.cm^{-2} and therefore a surface of membranes of at least $S_{membranes}$ = 16.3 cm^2 was needed. The good results obtained with TZFBR+MB configuration (2.46 mmol.min^{-1} of total H_2, $x_{CH4} = x_{CO2}$ = 0.39) confirm the concept but indicate that a bigger surface is required: p_{H2}= 190 mbar, *Sieverts*'s driving force of 11.3 mbar$^{0.5}$, 2.36 mL(STP). min^{-1}.cm^2 (Fig. 2), thus $S_{membranes}$ = 23.0 cm^2.

Effect of total height of the bed, h_0

According to these previous calculations, and taking into account that in configuration c1 (Fig. 3a) the membranes were not completely covered by the catalytic bed, we expected that an increase in the height of the bed would result in a further improvement of hydrogen production. To this end, a mass of 45 g of Al_2O_3 was added to the bed, as an inert solid, but maintaining the same total amount of catalyst in order to only increase the extent of membranes surface effective for hydrogen extraction. In this way, by doubling the height of the bed but maintaining the amount of catalyst, the reactor was operating under configurations b2 (FBR) and c2 (TZFBR+MB) of Figure 1. Figure 3b shows the evolution of hydrogen flow with time-on-stream in both configurations. As it could have been expected, a similar flow of hydrogen was obtained for FBR configuration regardless of the total height of the bed (b2 *vs.* b1). However, the higher the total height of the bed the higher the hydrogen over-yields when operating as a TZFBR+MB (c2 *vs.* c1), verifying that there was room for improvement by increasing the surface of membranes immersed in the bed. The total flow rate of hydrogen produced rose in more than a 40%, achieving approximately 3.5 mmol.min^{-1} (i.e., a fractional conversion of $x_{CH4} = x_{CO2} = 0.555$). For these news conditions p_{H2}= 250 mbar, *Sieverts*'s driving force of 13.4 mbar$^{0.5}$, 2.45 mL(STP). min^{-1}.cm^2 (Fig. 2), thus $S_{membranes}$ = 32.0 cm^2, that roughly corresponds with the total available surface of membranes.

We carried out, with configuration c2 (Figure 1), a series of experiments similar to the one which results have been shown in Figure 3b but varying the operating temperature (475-575°C). Figure 4 is a parity plot showing hydrogen yields for TZFBR+MB configuration (c2) against their FBR (b2) counterparts at different temperatures. Additionally, some results corresponding to shorter beds (configurations b1 and c1) are also shown for comparison purposes. As it can be seen, we obtained an important rise in hydrogen over-yields for the entire range of temperatures by doubling the height of the bed. So, for example, we achieved around a 100% of improvement at 575°C with TZFBR+MB over the FBR one, and around a 200% when working at 475°C (although at low temperatures the yield was considerably lower than at temperatures). Moreover, around 71% of the obtained hydrogen were pure hydrogen streams coming from the permeate side of the membrane. In particular, the percentages were 72.4%, 72.1%, 71.3%, 70.3%, and 70.3% for the five tested temperatures from 475°C to 575°C, respectively.

The good yields obtained from the last series allowed to verify the effectiveness of working with a larger bed that provides larger surface of membranes for hydrogen removal from the reacting atmosphere. Indeed, the thermodynamic equilibrium for the MDR reaction (r.1) was displaced by that hydrogen removal in the sense of producing more hydrogen, reaching noticeably superior conversions. Unfortunately, the larger the amount of H_2 removed through membranes, the more severe the coke production could be, and consequently the related catalyst deactivation. With regard to this concern about the stability of the process, it can be seen that in effect the drop of hydrogen flow over the time-on-stream seems to produce a more severe upshot for the largest TZFBR+MB bed (Figure 3). The first column of Table 2 shows the loss of activity in terms of percentage of variation of methane conversion (x_{CH4}) over the entire period of six hours working as TZFBR+MB, for each experiment. At high temperatures, over 500°C, there was a clear loss of activity, compatible with a neat increase of coke content on the surface of catalyst particles. This increase arises from the difference between, (i) the rate of coke formation throughout the reaction zone, and (ii) the rate of coke combustion throughout the regeneration zone. Since both rates increase with temperature, the instability presented a maximum at an intermediate temperature, 525°C for the experiments corresponding to Table 2.

Effect of relative height of the regeneration zone, z_0

In the light of the foregoing, we decided to increase the relative height of the regeneration zone (i.e., its ratio to the total bed height). To this end, the amount of Al_2O_3 in the bed was increased up to 63.75 g and the height of biogas feeding was set at 2.25 times its previous value, while maintaining the total load of catalyst and the rest of dimensions in the same values as before. The scheme c3 in Figure 1 represents this new arrangement of the reactor. As it can be seen in the second column of Table 2, the stability enhanced. This improvement was clearer at intermediate temperatures, for which there could be significant coke formation in the reaction zone and the kinetics of coke combustion was not fast enough to complete it in a short regeneration zone.

Figure 5 represents the evolution of methane conversion as a function of time-on-stream for the series of experiments carried out with both, z_0 and $2.25z_0$ as heights of the regeneration zone. Apart

from the gain in stability, slightly lower values of methane conversion were achieved for those experiments carried out with larger regeneration zone. This is due to the slightly higher dilution of catalyst particles in the bed with alumina particles. So, even though the height of the reaction zone was the same, its content in catalyst was marginally lower leading to the small drop in conversion. With regard to hydrogen yields, Figure 6 is an upgraded parity plot including the values obtained from the new series. Trends in percentage of improvement reached with TZFBR+MB arrangement are similar as before for all tested temperatures (i.e., from around +100% to +200% when working from 575°C to 475°C). Moreover, the permeate stream represented roughly 70% of the total obtained hydrogen for all tested temperatures, without great differences between them. Summarizing, increasing the height of the regeneration zone appeared as an affordable procedure, keeping good results in terms of over-yields in hydrogen production with respect to the FBR configuration, while counteracting more effectively the catalyst deactivation and so reaching a more stable global process.

Effect of partial pressure and nature of the oxidant agent

Another way to act on the regeneration step of the process is by changing the percentage and the nature of the regenerative agent. Therefore, we carried out a new series of experiments using different percentages of oxygen (with respect to the total gas stream fed to the reactor). We varied the oxygen content in the gas from 2.5% to 10% (Table 2). In the same way, we made some experiments using CO_2 as regenerative substance.

Figure 7 compares the evolution over time of hydrogen yields obtained from the experiments of this new series, working with z_0 and $2.25\ z_0$ as height of the regeneration zone. In general terms, the improvement for hydrogen yield using TZFBR+MB configuration is similar (notice the zoom in scale applied in TZFBR+MB results area) irrespective of the amount and nature of oxidant agent used. Thus, an average hydrogen yield of 54% was obtained against 26% for FBR configuration. In effect, these results correspond very closely with those presented in the parity plot (Figure 6) for the same temperature (550°C).

Regarding the stability of the system, when oxygen was used as regenerative agent, the higher its percentage the more stable was the process when working with a TZFBR+MB arrangement. However, no stabilization was achieved for any of the conditions used with the shorter regeneration zone while an apparent steady state was attained for p_{O2} = 0.100 bar and P_{O2} = 0.075 bar with the larger one. Regarding the use of carbon dioxide, we found necessary to work with a high partial pressure (p_{CO2} = 0.3 bar) and large regeneration zone (*2.25* z_0) to match the results with oxygen (in this case, with P_{O2} = 0.05). Clearly, given the lower capacity (according to the reaction stoichiometry) and the slower kinetics of carbon dioxide as oxidant, greater height of the regeneration zone and/or higher partial pressure would be required to reach a steady state.

In this sense, the weight of the carbonaceous deposits accumulated in the bed during the whole duration of the experiment (i.e., including the first two hours operating in a FBR configuration) can be analyzed from columns on the right side of Table 2. There was an apparent direct relationship between them and the unstable behavior of the system observed in Figure 7. However, the data for CO_2 with p_{CO2} = 0.3 bar and *2.25* z_0, far from presenting a similar value to that of the unstable experiment with P_{O2} = 0.05, actually was of the same magnitude as for those stable experiments with O_2 and p_{O2} = 0.100 and 0.075 bar. This evidence corresponds well to the evolution of the coke formation rate in the bed during the run. In effect, we estimated that rate from the mismatch in the carbon balance closure in the reactor for different time intervals (Figure 8). In all cases, the rate of coke formation was positive during the FBR period, leading to an important accumulation of coke in the fluidized bed. The accumulation rate was dropping as time passed because the catalyst surface progressively became saturated and simultaneously the reaction rate was decreasing. When we removed hydrogen through Pd/Ag membranes (TZFBR+MB period), the increase in the coke formation rate in the reaction zone of the bed was not sufficiently counteracted by its combustion in the regeneration zone, leading even to net rates of coke formation, even higher than those found during the FBR phase. This was especially true for the cases of lower height of the regeneration zone (z_0) and low partial pressure of the oxidants.

However, with a long regeneration zone (2.25 z_0) and high partial pressures of oxidant, the rate of coke combustion exceeded its rate of formation, producing even a negative rate that represented net consumption of coke. For example, in the case of p_{O2} = 0.100 bar this negative rate was reached very

early in the TZFBR+MB period and, consequently, at the end of the 8-hour experiment the system was practically in a dynamic equilibrium, with no net formation or net consumption of coke. For CO_2 with p_{CO2} = 0.3 bar, the aftermath appeared later, presenting a temporary gap with respect the aforementioned case, but also showing a tendency to reach a similar state of dynamic equilibrium with a low amount of coke in the bed. In this regard, it can be seen the low value (164 mg) reached for 8 h of experiment (Table 2), taking into account that there was an accumulation of coke in the bed even in the first 3 hours of TZFBR+MB operation.

Therefore, it can be established that CO_2 can be used as a regenerative agent for this process and that a suitable amount of CO_2 results in similar stability to using O_2 as regenerative agent. Moreover, in some occasions CO_2 could be preferable for the safety point of view. Nevertheless, there is an additional safeguard to be taken into account when working with a TZFBR+MB configuration using oxygen as catalyst regenerating agent. On the one hand, a high partial pressure of oxygen in the stream fed to the regeneration zone favors, as aforementioned, the elimination of coke and consequently the stability of the process. However, on the other hand, if there is an excess of oxygen, it could reach the reaction zone. Then, in addition to produce the undesired oxidation of some part of CH_4, CO or H_2, this oxygen could lead to the oxidation of the metallic active phase of the catalyst (Ni, and Ce) and gradually to its deactivation [27, 28]. This behavior was observed when long lasting experiments were carried out. As an example, Figure 9 shows the temporal evolution of methane conversion in a TZFBR+MB reactor for three different partial pressures of O_2 or CO_2 as oxidant agents. Although a greater conversion was kept from the beginning with a partial pressure of oxygen of p_{O2} = 0.100 bar, since the second day of operation there was an abrupt drop in activity attributable to the oxidation of the active phase of the catalyst. Using lower partial pressures of oxygen (p_{O2} = 0.05) or using carbon dioxide (p_{CO2} = 0.30), the process remained more stable for the entire duration of these runs. It can also be observed that, at the beginning of each day (after a night without reaction and with inert gas flowing through the reactor) there was a slight upturn in activity that can be attributed to the cleaning of catalyst and membranes produced overnight.

Effect of not including an activation period

In this context, to avoid a more oxidant atmosphere in which the metal is oxidized and consequently decays in activity, [24] established the need to start the process without hydrogen extraction for some time before using the membranes. In this way, it was implemented an 'activation period' in which the system was working with configuration c1 but without hydrogen extraction. The effect of removing this preliminary period was analyzed with the new arrangement settled in this work, configuration c3. Thus, Figure 10 presents the comparison of hydrogen yields obtained with or without activation period, working with three different partial pressures of oxygen. As it can be seen, no differences were obtained by removing the activation period. That implies that the system, with its new arrangement (configuration c3) can be started in his TZFBR+MB mode without getting penalized in terms of activity or stability of the process.

Comparison with the literature

We demonstrated [24] that a TZFBR+MB offers an interesting increase in the overall selectivity to hydrogen at 500°C, not only in relation to their own FBR findings but also in relation to other published results. Figure 11 shows an updated version of that comparison including more bibliographic results as well as the findings of this work, all of them for Ni-based catalysts. In the same way, comparative results for the temperature of 550°C are also shown in this Figure. In conventional FBR, as well as in other conventional reactors used in bibliography (mostly fixed bed reactors), the H_2/CO ratio was roughly the one that could be achieved according to the thermodynamic equilibrium regardless of the methane conversion. Moreover, this methane conversion was always equal to or lower than the one for equilibrium estimated for gas phase at the working temperature (except for the works of *Aghamohammadi et al.* [29] and *Damyanova et al.* [30], working at 550°C and using catalysts containing Ce).

Noticeably, the use of TZFBR+MB configurations greatly increases both methane conversion and H_2/CO ratio, even well over the limit given by the thermodynamic equilibrium in a conventional reactor.

In this sense, the values obtained in this work markedly overperform earlier results [24] which were obtained in a TZFBR+MB configuration without the upgrading of the operating conditions and arrangement carried out in this work. Moreover, and contrarily what happens in the systems with which the comparison is made, the proposed TZFBR+MB system is stable because catalyst regeneration is taking place simultaneously. Additionally, no alterations in membranes performance were observed after using them in MDR reaction for around 900 hours. A good repeatability for the experimental measurements was observed.

CONCLUSIONS

Former hydrogen over-yields [24], offered by a TZFBR-MB reactor configuration versus a conventional FBR one, are improved when working with greater bed height and more effective membrane permeation surface. Values from around +100% to +200% are reached in the temperature interval from 575°C to 475°C (Figure 4).

Although the larger hydrogen flow extracted under those conditions has the negative effect of producing more coke (Table 2), enlarging the relative height of the oxidation zone (i.e., the ratio z/h) effectively counteracts this trend and allows the reactor to recover stability (Figure 5) whilst maintaining the levels of hydrogen over-yields (Figure 6). Moreover, when high partial pressures of oxidant (O_2 or CO_2) are used coke combustion rate is favoured, exceeding its formation rate (Figure 8), and so a better stability is reached (Figure 7). However, if there is an excess of oxygen, it lead to the oxidation of the metallic active phase of the catalyst (Ni, and Ce) and gradually to its deactivation (Figure 9). Finally, the system with this new arrangement (higher values of bed height, ratio z/h and p_{O2}) can be started in the TZFBR+MB mode without getting penalized in terms of activity or stability (Figure 10).

TZFBR+MB configuration for MDR greatly increases methane conversion and hydrogen selectivity (expressed as H_2/CO ratio), overperforming bibliographic results, even well over the limit given by the thermodynamic equilibrium in a conventional reactor (Figure 11). Additionally, with configurations

adopted in this work great part of the H_2 (70-80%) is obtained with a high degree of purity and could therefore be employed in cases where such purity is essential, for example in fuel cells.

The proposed system, although with a limited mass flux (u_{mf} can be only slightly exceeded), provides an interesting tool of process integration and stable operation in which the improvement/optimization of operating conditions has given high performance results in terms of hydrogen yields.

ACKNOWLEDGEMENTS

Financial support for this work has been provided by the Spanish *Ministerio de Economía y Competitividad* (MINECO), through project ENE2013-44350-R.

REFERENCES

[1] C.S. Lau, A. Tsolakis, M.L. Wyszynski, Biogas upgrade to syn-gas (H_2-CO) via dry and oxidative reforming, Int. J. Hydrogen Energy. 36 (2011) 397–404. doi:10.1016/j.ijhydene.2010.09.086.

[2] D. Deublein, A. Steinhauser, Biogas from Waste and Renewable Resources, 2nd Revised and Expanded Edition, Wiley-VCH, Germany, 2010.

[3] X. Chen, H. Vinh, A. Avalos Ramirez, D. Rodrigue, S. Kaliaguine, Membrane gas separation technologies for biogas upgrading, RSC Adv. 5 (2015) 24399-24448. doi: 10.1039/C5RA00666J.

[4] M. Hafttananian, A. Ramiar, B. Shabani, A.A. Ranjbar, Nonlinear algorithm of PEM fuel cell catalyst poisoning progress in the presence of carbon monoxide in anode fuel: A computational study using OpenFOAM, Electrochim. Acta. 246 (2017) 348–364. doi:10.1016/j.electacta.2017.06.021.

[5] S.T. Oyama, P. Hacarlioglu, Y. Gu, D. Lee, Dry reforming of methane has no future for hydrogen production: Comparison with steam reforming at high pressure in standard and membrane reactors, Int. J. Hydrogen Energy. 37 (2012) 10444–10450. doi:10.1016/j.ijhydene.2011.09.149.

[6] T. Chompupun, S. Limtrakul, T. Vatanatham, C. Kanhari, P.A. Ramachandran, Experiments, modeling and scaling-up of membrane reactors for hydrogen production via steam methane reforming, Chem. Eng. Process. - Process Intensif. 134 (2018) 124–140. doi:10.1016/j.cep.2018.10.007.

[7] G. Di Marcoberardino, S. Foresti, M. Binotti, G. Manzolini, Potentiality of a biogas membrane reformer for decentralized hydrogen production, Chem. Eng. Process. - Process Intensif. 129 (2018) 131–141. doi:10.1016/j.cep.2018.04.023.

[8] B. Anzelmo, J. Wilcox, S. Liguori, Hydrogen production via natural gas steam reforming in a Pd-Au membrane reactor. Investigation of reaction temperature and GHSV effects and long-term stability, J. Memb. Sci. 565 (2018) 25–32. doi:10.1016/j.memsci.2018.07.069.

[9] B. Anzelmo, J. Wilcox, S. Liguori, Hydrogen production via natural gas steam reforming in a Pd-

Au membrane reactor. Comparison between methane and natural gas steam reforming reactions, J. Memb. Sci. 568 (2018) 113–120. doi:10.1016/j.memsci.2018.09.054.

[10] J.D. Silva, C.A.M. de Abreu, Modelling and simulation in conventional fixed-bed and fixed-bed membrane reactors for the steam reforming of methane, Int. J. Hydrogen Energy. 41 (2016) 11660–11674. doi:10.1016/j.ijhydene.2016.01.083.

[11] B. Dittmar, A. Behrens, N. Schödel, M. Rüttinger, T. Franco, G. Straczewski, R. Dittmeyer, Methane steam reforming operation and thermal stability of new porous metal supported tubular palladium composite membranes, Int. J. Hydrogen Energy. 38 (2013) 8759–8771. doi:10.1016/j.ijhydene.2013.05.030.

[12] E. Fernandez, A. Helmi, K. Coenen, J. Melendez, J.L. Viviente, D.A. Pacheco Tanaka, M. van Sint Annaland, F. Gallucci, Development of thin Pd–Ag supported membranes for fluidized bed membrane reactors including WGS related gases, Int. J. Hydrogen Energy. 40 (2015) 3506–3519. doi:10.1016/j.ijhydene.2014.08.074.

[13] S.A. Wassie, J.A. Medrano, A. Zaabout, S. Cloete, J. Melendez, D.A.P. Tanaka, S. Amini, M. van Sint Annaland, F. Gallucci, Hydrogen production with integrated CO_2 capture in a membrane assisted gas switching reforming reactor: Proof-of-Concept, Int. J. Hydrogen Energy. 43 (2018) 6177–6190. doi:10.1016/j.ijhydene.2018.02.040.

[14] S.A. Wassie, S. Cloete, V. Spallina, F. Gallucci, S. Amini, M. van Sint Annaland, Techno-economic assessment of membrane-assisted gas switching reforming for pure H_2 production with CO_2 capture, Int. J. Greenh. Gas Control. 72 (2018) 163–174. doi:10.1016/j.ijggc.2018.03.021.

[15] D. Zambrano, J. Soler, J. Herguido, M. Menéndez, Kinetic Study of Dry Reforming of Methane over Ni-Ce/Al_2O_3 Catalyst with Deactivation, Top. Catal. (2019). doi: 10.1007/s11244-019-01157-2.

[16] J. Herguido, M. Menéndez, J. Santamaría, On the use of fluidized bed catalytic reactors where reduction and oxidation zones are present simultaneously, Catal. Today. 100 (2005) 181–189. doi:10.1016/j.cattod.2004.11.004.

[17] J. Herguido, M. Menéndez, Advances and trends in two-zone fluidized-bed reactors, Curr. Opin. Chem. Eng. 17 (2017) 15–21. doi:10.1016/j.coche.2017.05.002.

[18] C.S. Patil, M. van Sint Annaland, J.A.M. Kuipers, Fluidised bed membrane reactor for ultrapure hydrogen production via methane steam reforming: Experimental demonstration and model validation, Chem. Eng. Sci. 62 (2007) 2989–3007. doi:10.1016/j.ces.2007.02.022.

[19] Z. Chen, J.R. Grace, C. Jim Lim, A. Li, Experimental studies of pure hydrogen production in a commercialized fluidized-bed membrane reactor with SMR and ATR catalysts, Int. J. Hydrogen Energy. 32 (2007) 2359–2366. doi:10.1016/j.ijhydene.2007.02.036.

[20] M.P. Gimeno, Z.T. Wu, J. Soler, J. Herguido, K. Li, M. Menéndez, Combination of a Two-Zone Fluidized Bed Reactor with a Pd hollow fibre membrane for catalytic alkane dehydrogenation, Chem. Eng. J. 155 (2009) 298–303. doi:10.1016/j.cej.2009.06.037.

[21] J.A. Medrano, I. Julián, J. Herguido, M. Menéndez, Pd-Ag membrane coupled to a two-zone fluidized bed reactor (TZFBR) for propane dehydrogenation on a Pt-Sn/$MgAl_2O_4$ catalyst, Membranes (Basel). 3 (2013) 69–86. doi:10.3390/membranes3020069.

[22] J.A. Medrano, I. Julián, F.R. García-García, K. Li, J. Herguido, M. Menéndez, Two-zone fluidized bed reactor (TZFBR) with palladium membrane for catalytic propane dehydrogenation: Experimental performance assessment, Ind. Eng. Chem. Res. 52 (2013) 3723–3731. doi:10.1021/ie303185p.

[23] H. Montesinos, I. Julián, J. Herguido, M. Menéndez, Effect of the presence of light hydrocarbon mixtures on hydrogen permeance through Pd-Ag alloyed membranes, Int. J. Hydrogen Energy. 40 (2015) 3462–3471. doi:10.1016/j.ijhydene.2014.11.054.

[24] P. Ugarte, P. Durán, J. Lasobras, J. Soler, M. Menéndez, J. Herguido, Dry reforming of biogas in fluidized bed: Process intensification, Int. J. Hydrogen Energy. 42 (2017) 13589–13597. doi:10.1016/j.ijhydene.2016.12.124.

[25] J. Lachén, P. Durán, M. Menéndez, J.A, Peña, J. Herguido, Biogas to high purity hydrogen by

methane dry reforming in TZFBR+MB and exhaustion by Steam-Iron Process. Techno-economic assessment, Int. J. Hydrogen Energy, 43 (2018) 11663-11675. doi:10.1016/j.ijhydene.2018.03.105

[26] P. Djinović, A. Pintar, Stable and selective syngas production from dry CH_4-CO_2 streams over supported bimetallic transition metal catalysts, Appl. Catal. B Environ. 206 (2017) 675–682. doi:10.1016/j.apcatb.2017.01.064.

[27] C. Wang, N. Sun, N. Zhao, W. Wei, Y. Sun, C. Sun, Coking and deactivation of a mesoporous Ni–CaO–ZrO2 catalyst in dry reforming of methane: A study under different feeding compositions, Fuel, 143 (2015) 527-535. doi:10.1016/j.fuel.2014.11.097

[28] Z. Hou, J. Gao, J. Guo, D. Liang, H. Lou, X. Zheng, Deactivation of Ni catalysts during methane autothermal reforming with CO_2 and O_2 in a fluidized-bed reactor, J. Catal., 250 (2007) 331-341. doi: 10.1016/j.jcat.2007.06.023

[29] S. Aghamohammadi, M. Haghighi, M. Maleki, N. Rahemi, Sequential impregnation vs. sol-gel synthesized Ni/Al_2O_3-CeO_2 nanocatalyst for dry reforming of methane: Effect of synthesis method and support promotion, Mol. Catal. 431 (2017) 39–48. doi:10.1016/j.mcat.2017.01.012.

[30] S. Damyanova, B. Pawelec, R. Palcheva, Y. Karakirova, M.C. Capel-Sanchez, G. Tyuliev, E. Gaigneaux, J.L.G. Fierro, Structure and surface properties of ceria-modified Ni-based catalysts for hydrogen production, Appl. Catal. B Environ. 225 (2018) 340–353. doi:10.1016/j.apcatb.2017.12.002.

[31] M.E. Gálvez, A. Albarazi, P. Da Costa, Enhanced catalytic stability through non-conventional synthesis of Ni/SBA-15 for methane dry reforming at low temperatures, Appl. Catal. A Gen. 504 (2015) 143–150. doi:10.1016/j.apcata.2014.10.026.

[32] B. Steinhauer, M.R. Kasireddy, J. Radnik, A. Martin, Development of Ni-Pd bimetallic catalysts for the utilization of carbon dioxide and methane by dry reforming, Appl. Catal. A Gen. 366 (2009) 333–341. doi:10.1016/j.apcata.2009.07.021.

[33] A. Serrano-Lotina, L. Daza, Highly stable and active catalyst for hydrogen production from biogas, J. Power Sources. 238 (2013) 81–86. doi:10.1016/j.jpowsour.2013.03.067.

[34] M.M. Barroso-Quiroga, A.E. Castro-Luna, Catalytic activity and effect of modifiers on Ni-based catalysts for the dry reforming of methane, Int. J. Hydrogen Energy. 35 (2010) 6052–6056. doi:10.1016/j.ijhydene.2009.12.073.

[35] L. Yao, Y. Wang, J. Shi, H. Xu, W. Shen, C. Hu, The influence of reduction temperature on the performance of ZrO_x/Ni-MnO_x/SiO_2 catalyst for low-temperature CO_2 reforming of methane, Catal. Today. 281 (2017) 259–267. doi:10.1016/j.cattod.2016.05.031.

[36] R. Dębek, M. Motak, M.E. Galvez, T. Grzybek, P. Da Costa, Promotion effect of zirconia on Mg(Ni,Al)O mixed oxides derived from hydrotalcites in CO_2 methane reforming, Appl. Catal. B Environ. 223 (2018) 36–46. doi:10.1016/j.apcatb.2017.06.024.

FIGURE CAPTIONS

Figure 1. Scheme and different configurations for used reactors. (a) Scheme of a two-zone fluidized bed reactor using permselective membranes and its main streams. (b) co-feeding configurations (conventional FBR) . (c) TZFBR+MB configurations.

Figure 2. Hydrogen permeating flux vs. *Sieverts*' driving force for Pd-Ag membranes at different temperatures. Q_{H2} = 80 STP mL.min^{-1}. $S_{membranes}$ = 30.6 cm^2. $p_{permeate}$ = 6 mbar.

Figure 3. Flowrate (mmol/min) of produced hydrogen as a function of time-on-stream and reactor configuration: (a) changing from configuration b1 to c1, (b) from b2 to c2. Experimental conditions as in Table 1.

Figure 4. Parity plot of hydrogen yields for TZFBR+MB configuration (c2) against their FBR (b2) counterparts at different temperatures. Small gray symbols correspond to configuration c2 against b1: *[a]* work of *Ugarte et al.*[24]; *[b]* this work. Experimental conditions as in Table 1.

Figure 5.- Methane conversion as a function of time-on-stream and reaction temperature, changing reactor configuration from: (i) b2 to c2 (empty symbols and discontinuous lines), (ii) b2 to c3 (full symbols and continuous lines). Experimental conditions as in Table 1.

Figure 6. Parity plot of hydrogen yields for TZFBR+MB configuration (c3) against their FBR (b2) counterparts at different temperatures. Small gray symbols correspond to configuration c2 against b2 from Figure 4. Experimental conditions as in Table 1.

Figure 7. Hydrogen yield as a function of time-on-stream and partial pressure of oxidant agent, changing reactor configuration from: (a) b2 to c2 (empty symbols and discontinuous lines), (b) b2 to c3 (full symbols and continuous lines). Experimental conditions as in Table 1.

Figure 8. Rate of coke formation (mg.min^{-1}) over time-on-stream for the experiments of Figure 7.

Figure 9. Methane conversion through time-on-stream for long lasting experiments in TZFBR+MB (configuration c3) and three different partial pressures of O_2 or CO_2. Rest of experimental conditions as in Table 1.

Figure 10. Comparison of hydrogen yields obtained in the conditions of Fig. 7b with their equivalents without the initial 2 hour period working as FBR.

Figure 11. H_2/CO ratio in the global outlet gas stream. Comparison with previous studies using similar temperatures (500°C and 550°C) and feed ratios (CH_4/CO_2 = 1).

Table 1.- Experimental conditions for a standard MDR test

Variable (units)	***Base value (studied range)***	
T (°C)	550 (475-575)	
$W_{o\ \text{catalyst}}$ (g)	30	
$W_{o\ \text{alumina}}$ (g)	0 (0, 45, 63.75)	
q_{total} gas (STP mL/min)	235.5	
Gas composition (%vol)	[FBR]	[TZFBR]
	CH_4: 30 CO_2: 30 N_2: 5 O_2: - Ar: 35	CH_4: 30 CO_2: 30 N_2: 5 O_2: 10 (2.5-10) Ar: 25 (32.5- 25)
$u_{r,\ \text{regeneration}}$ (-)	1.2	
$u_{r,\ \text{reaction}}$ (-)	3.0	
z_0 *(cm) – Fig. 1-*	2	
h_0 *(cm) – Fig. 1-*	15	

Table 2.- Increase in methane conversion (ΔX_{CH4}) and in the amount of coke formed (ΔW_{Coke}) during the course of different experiments (i.e., modifying height of the regeneration zone, *T*, and $p_{oxidant}$)

T (°C)	ΔX_{CH4} (%)*			$P_{oxidant}$ (bar)	ΔW_{Coke} (mg)**	
	z_0	$2.25.z_0$			z_0	$2.25.z_0$
475	+1.2	+4.9		**0.100 O_2**	693	56
500	+0.4	+12.5		**0.075 O_2**	1,240	326
525	-3.7	+4.5		**0.050 O_2**	2,115	1,547
550	-1.2	-0.2				
575	-1.5	-1.5		**0.300 CO_2**	2,781	164

* during the TZFBR+MB period (Figure 5)

** during the entire duration of the experiment (Figure 7)

Graphical Abstract

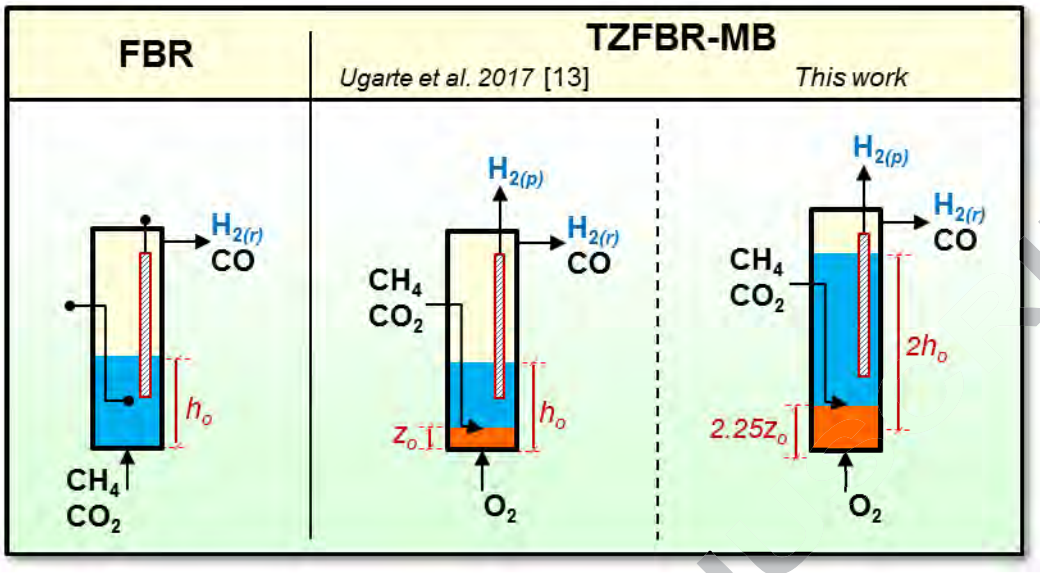

Pure hydrogen from biogas: intensified methane dry reforming in a two-zone fluidized bed reactor using permselective membranes

P. Durán, A. Sanz, J. Soler, M. Menéndez, J. Herguido*

Suggested highlights:

- Process intensification in a two zone fluidized bed with H_2 permselective membranes
- Concurrent CH_4 dry reforming, catalyst regeneration and H_2 separation are achieved
- 70-85% of hydrogen is obtained as a pure (membrane permeate) stream
- Stable behaviour can be reached by modifying reactor configuration
- CH_4 conversions and H_2/CO ratios exceed the limits of conventional reactors

Figure 01

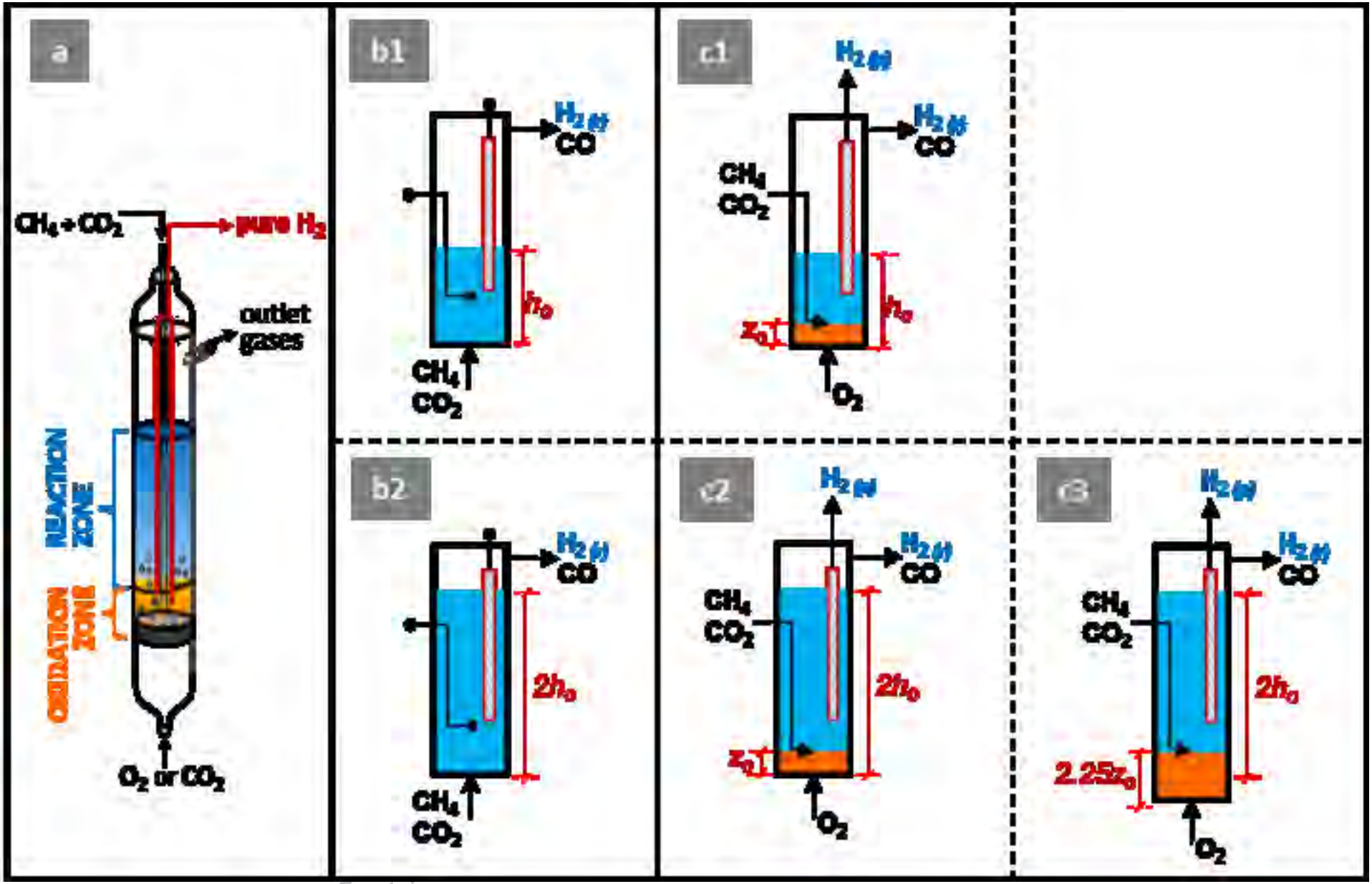

Figure 02

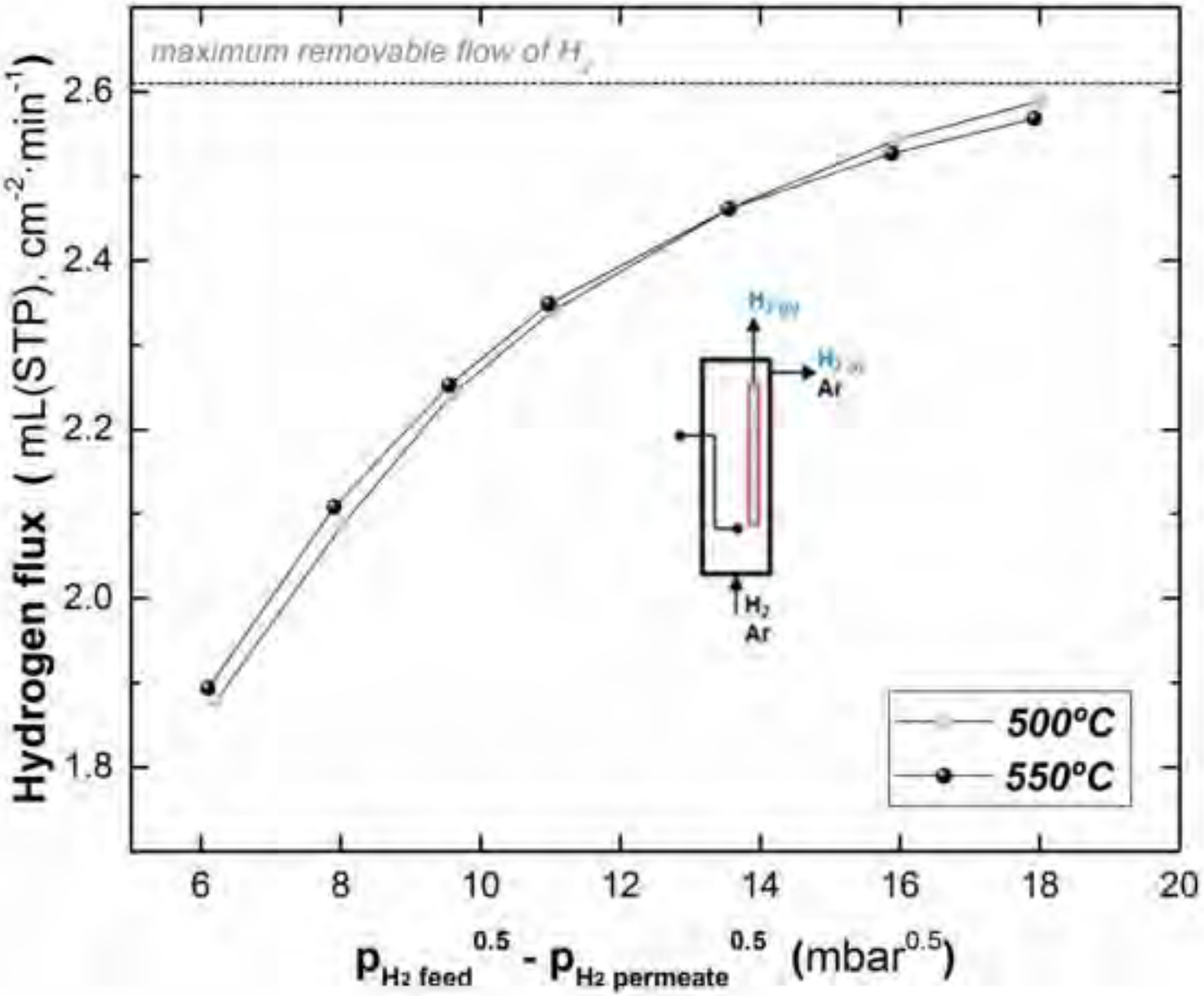

Figure 03a

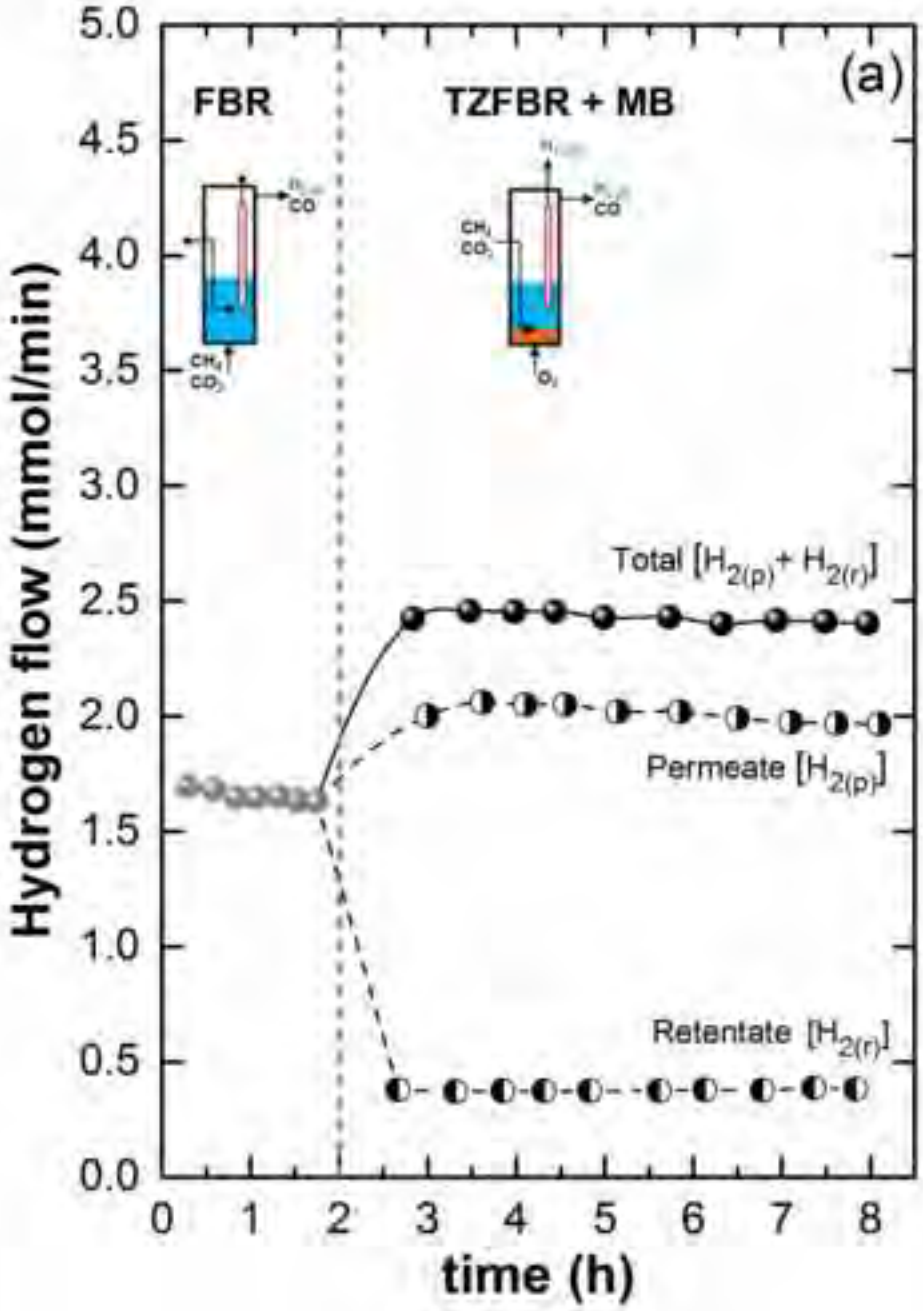

Figure 03b

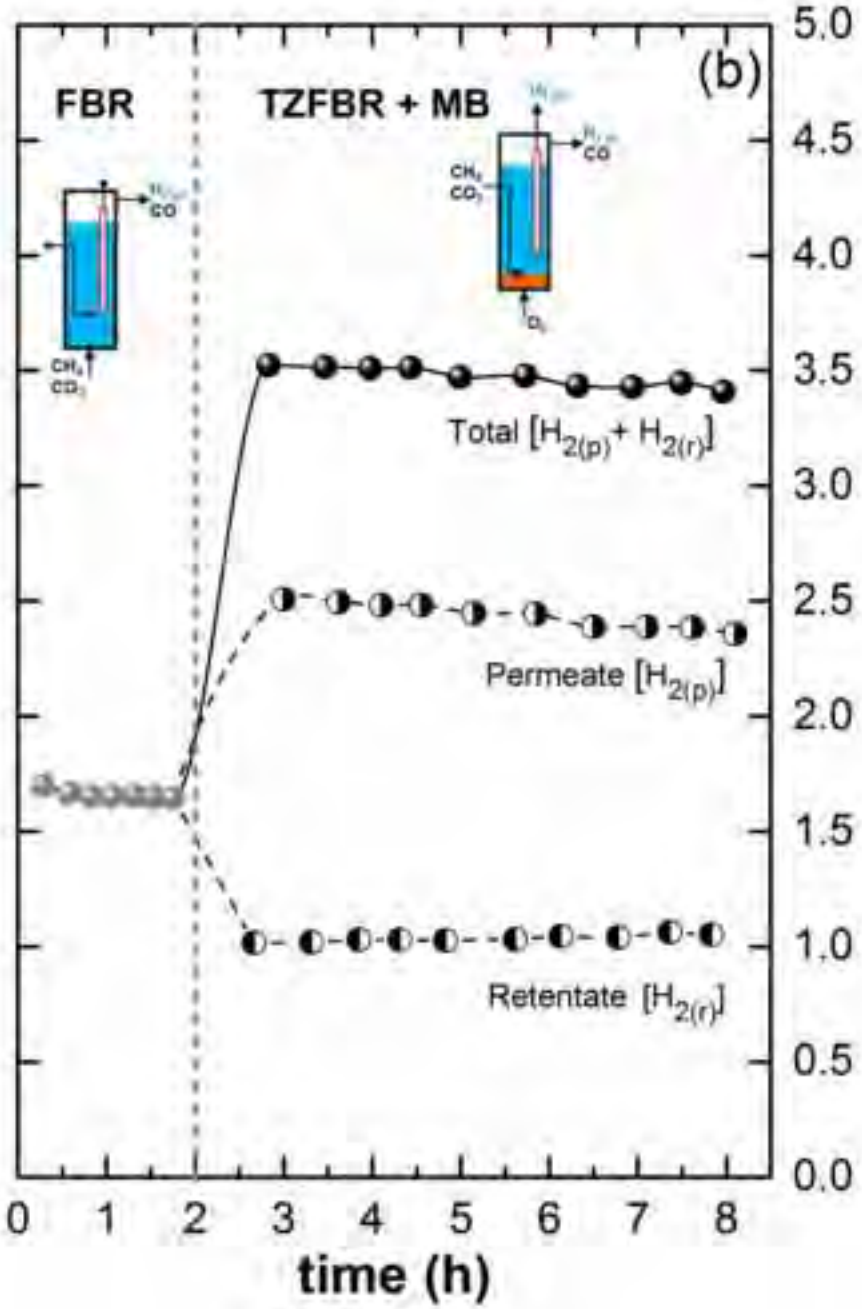

Figure 03 - presentation scheme (pdf format)

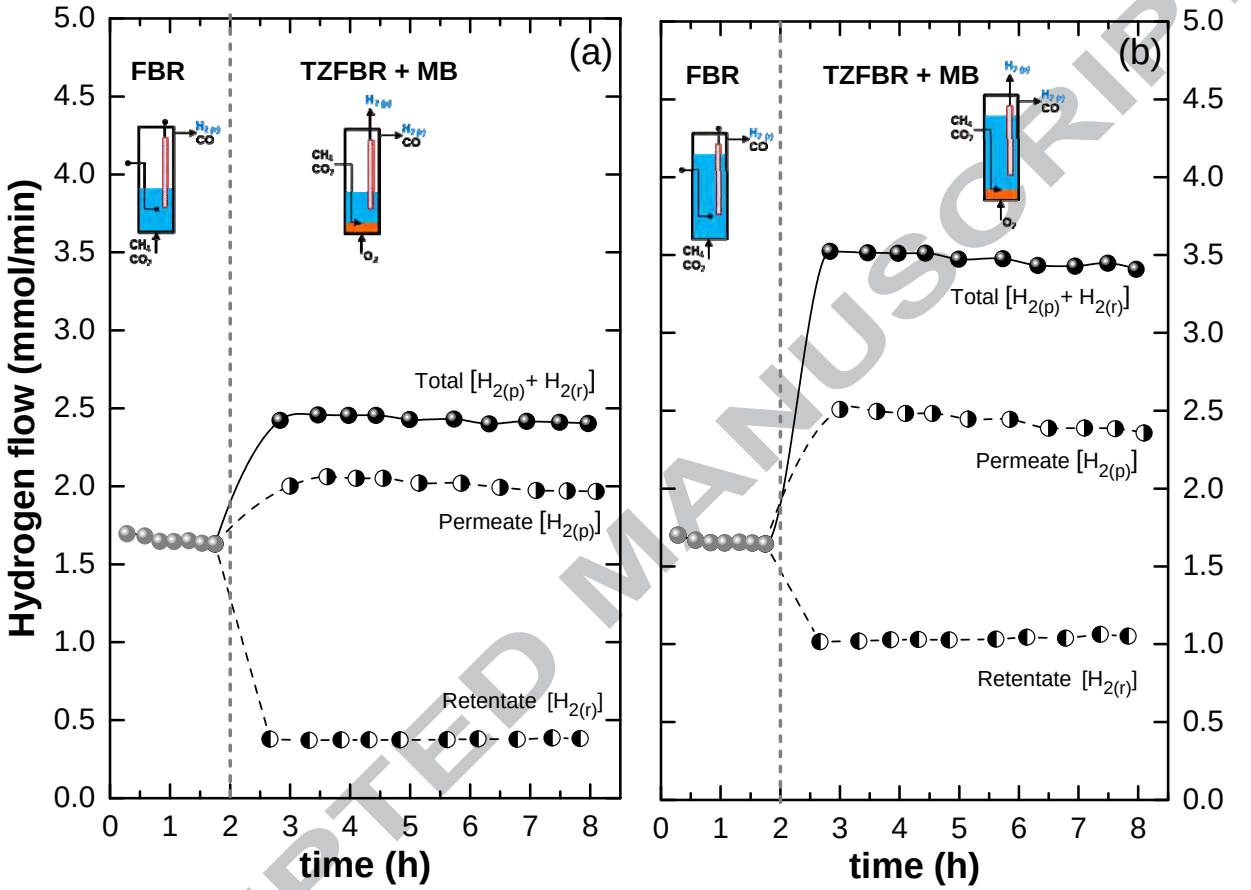

Figure 04

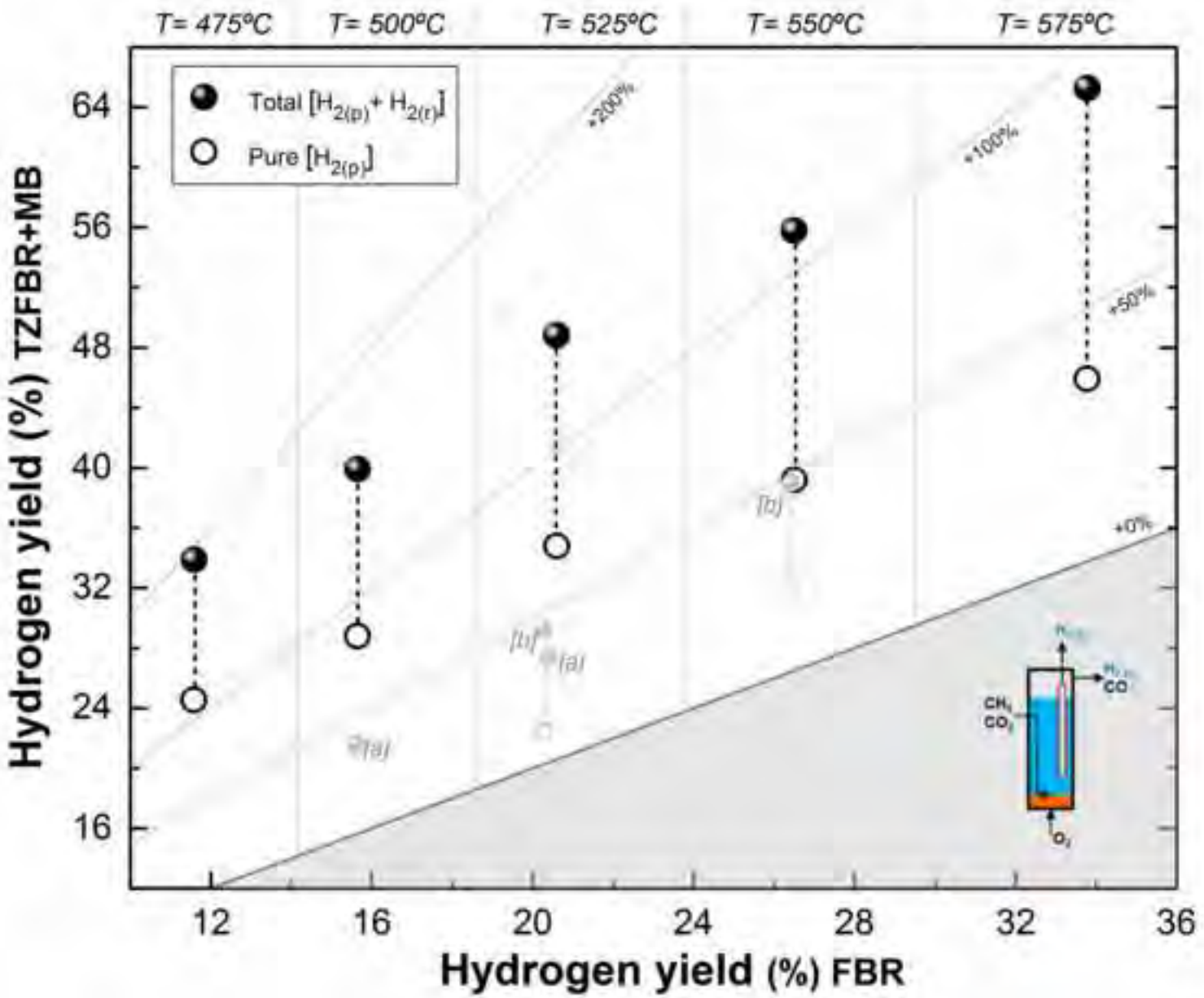

Figure 05

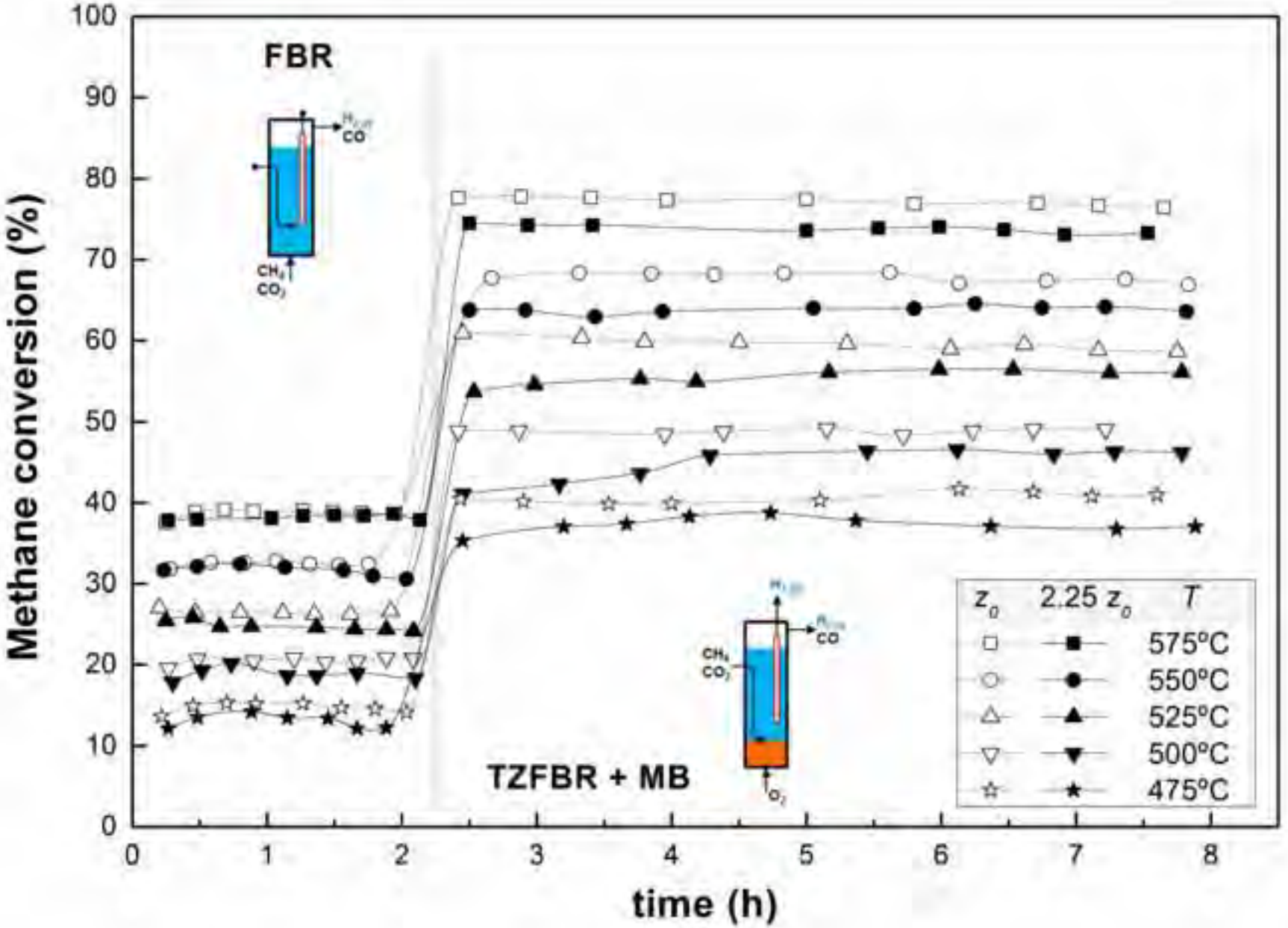

Figure 06

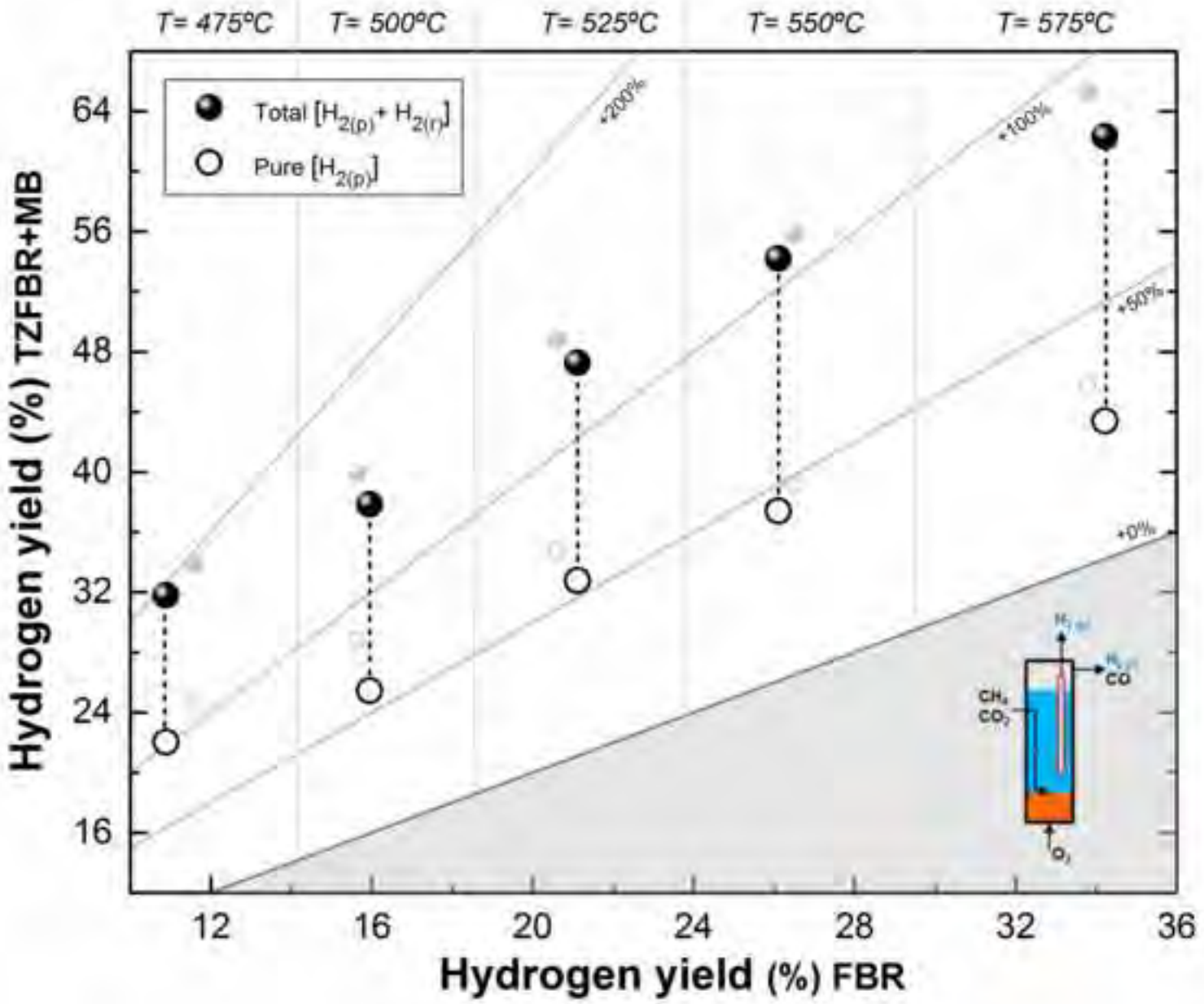

Figure 07a

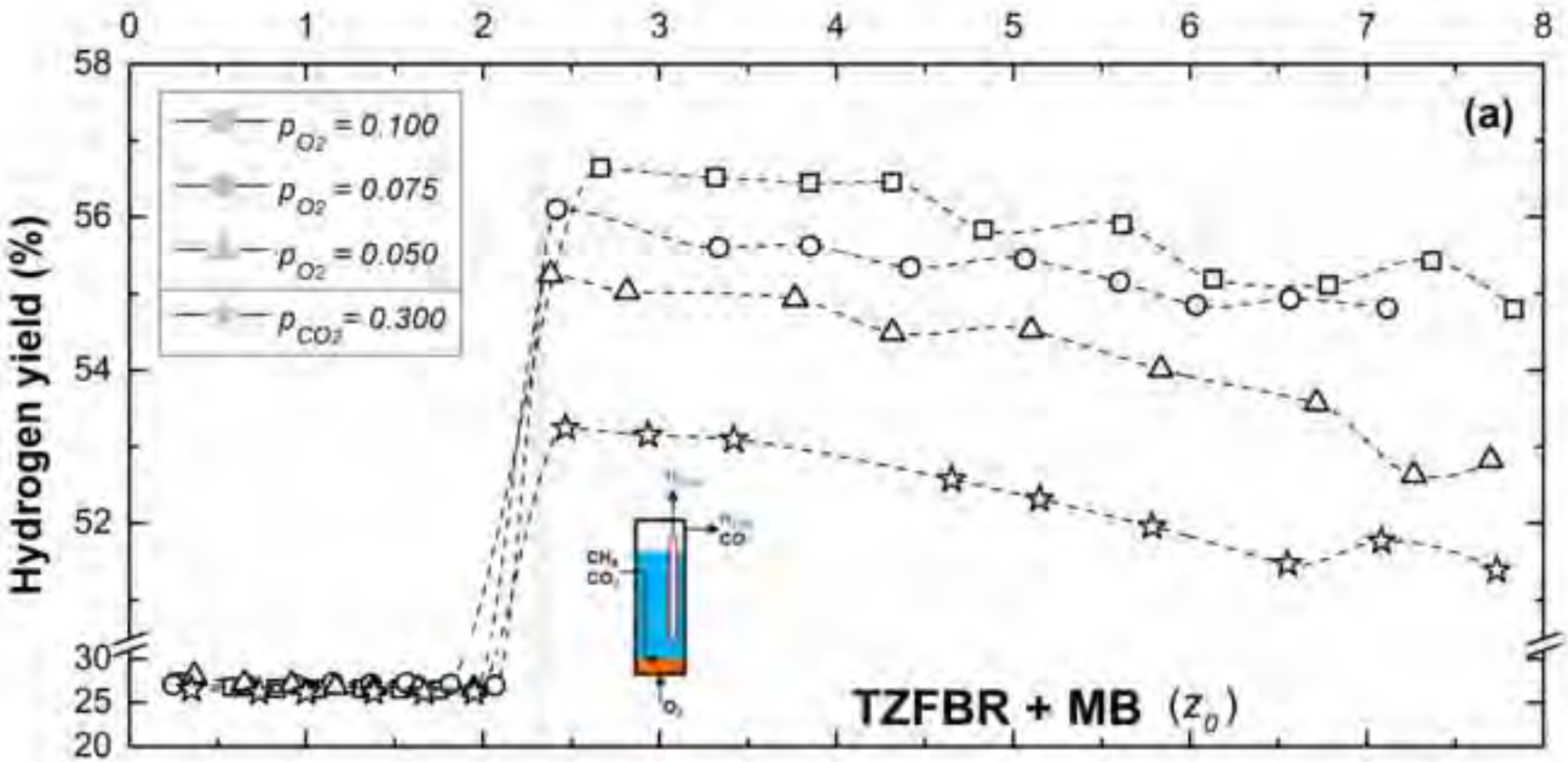

Figure 07b

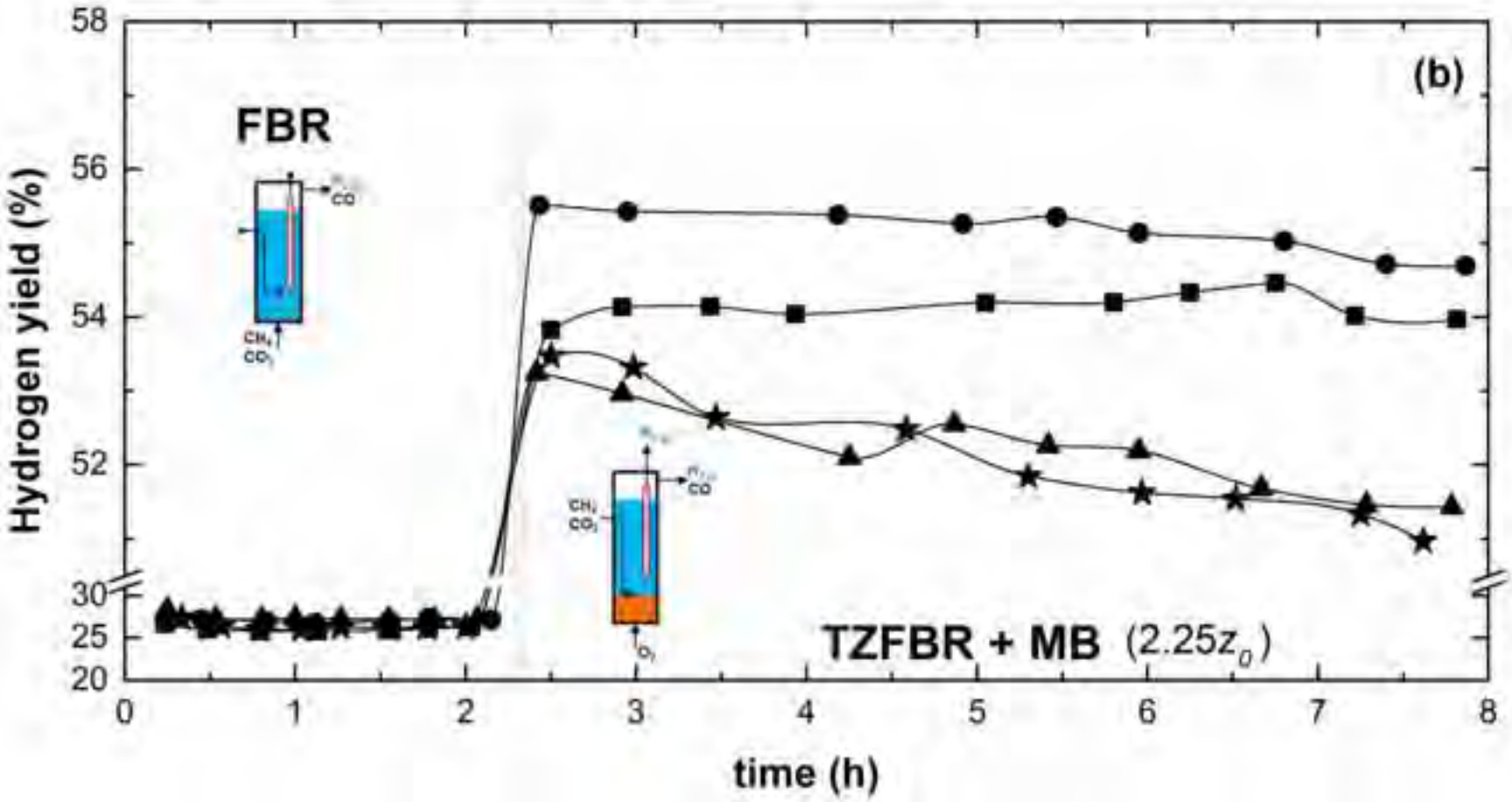

Figure 07 - presentation scheme (pdf format)

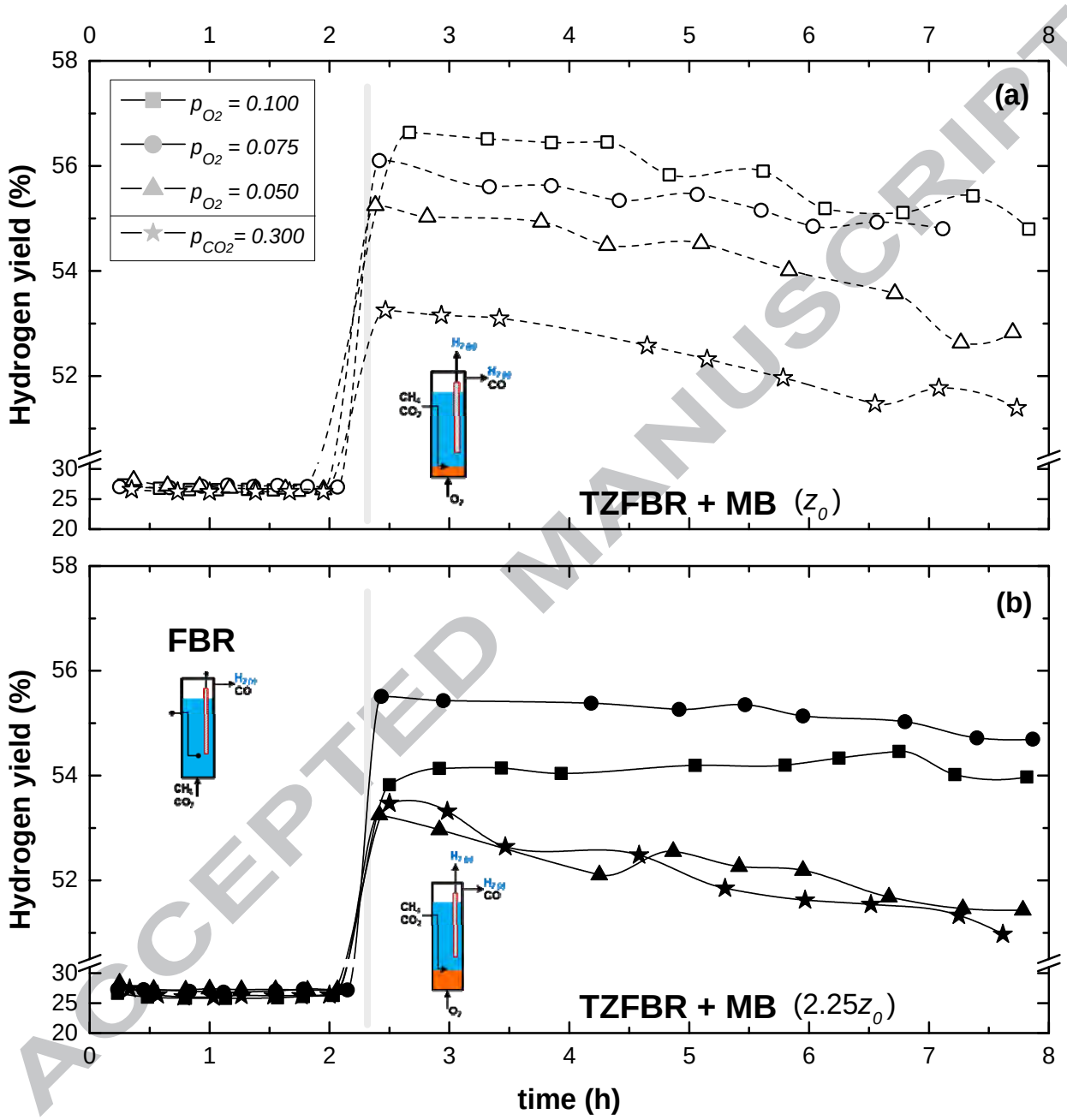

Figure 08

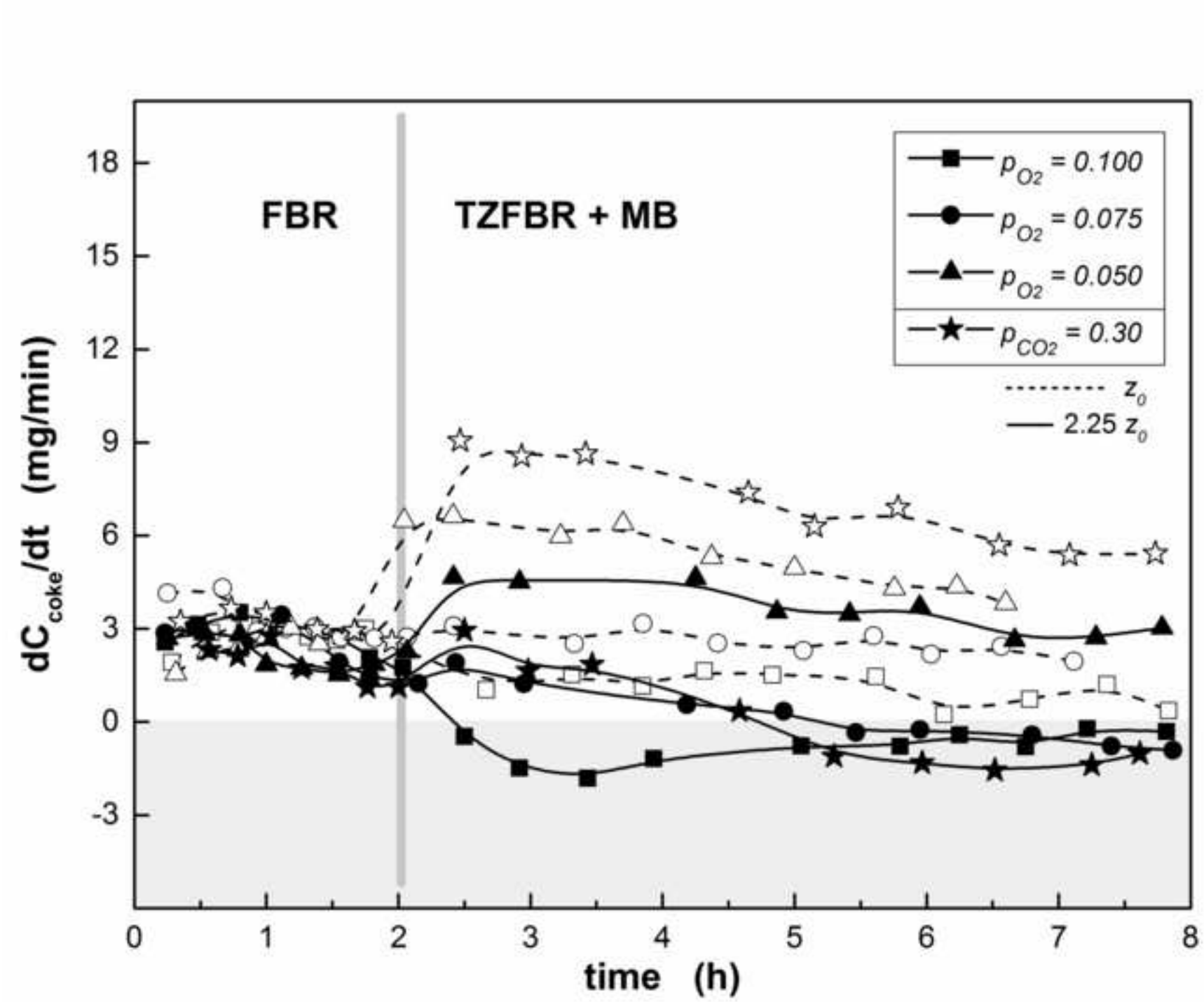

Figure 09

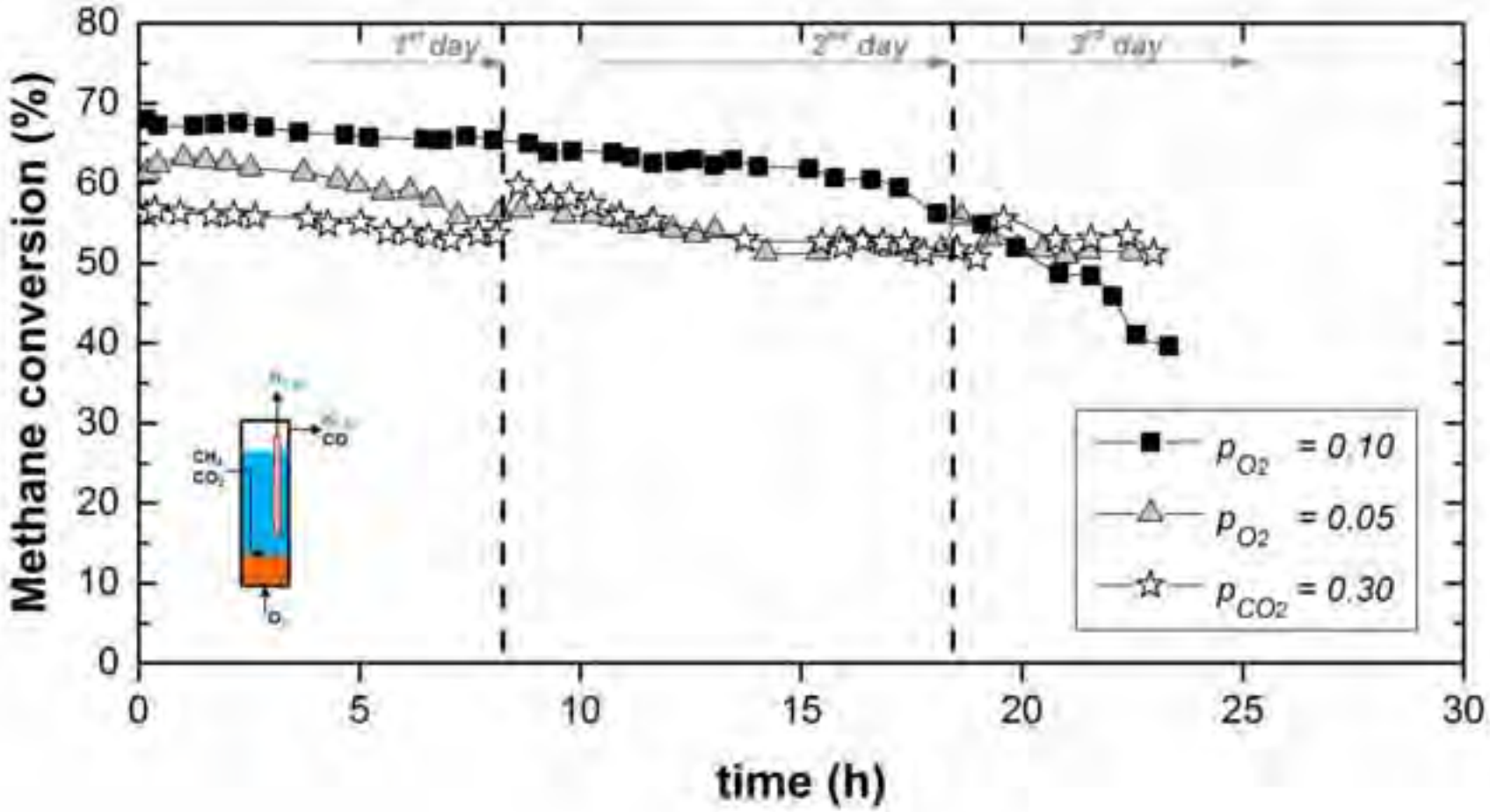

Figure 10

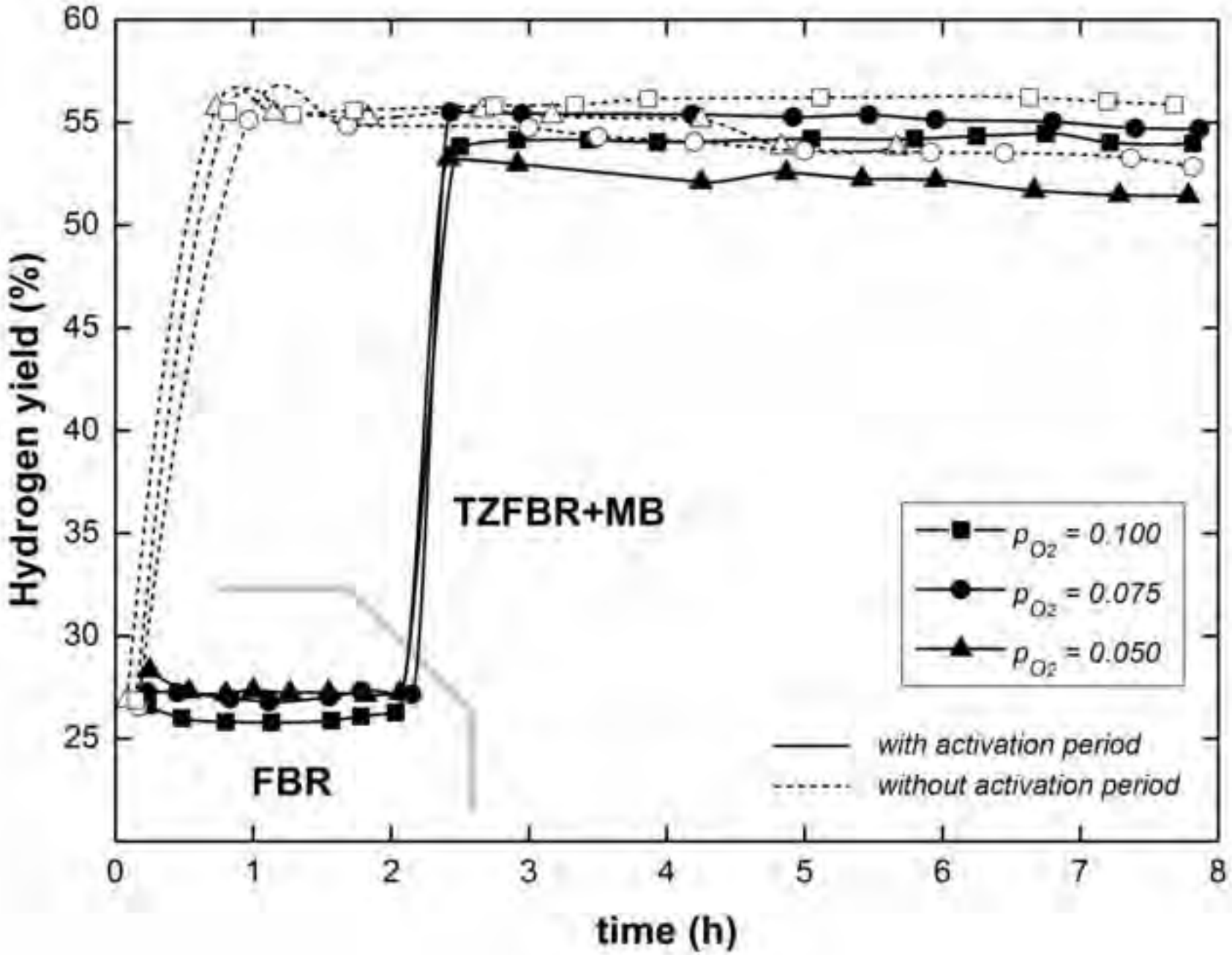

Figure 11a (revised)

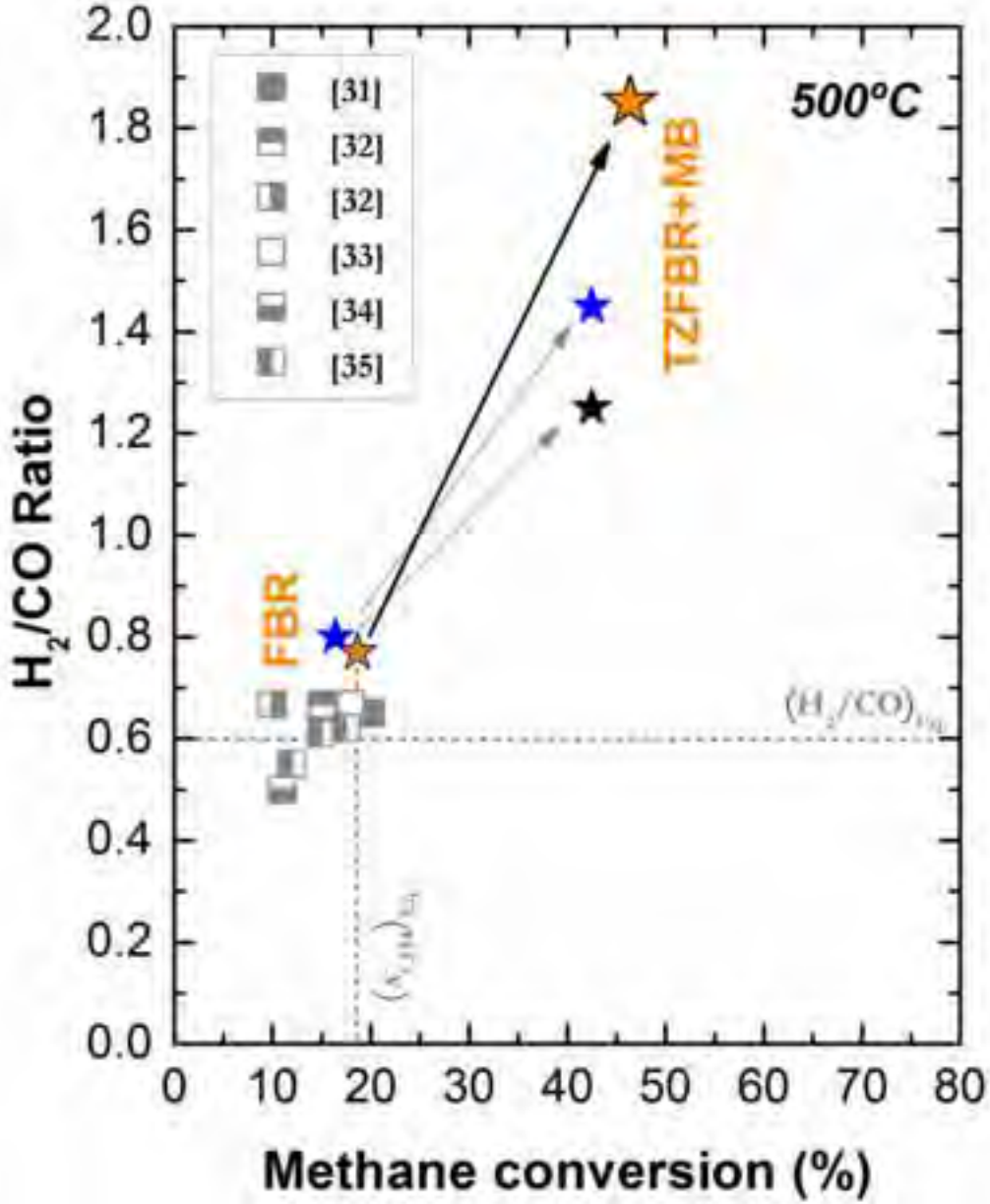

Figure 11b (revised)

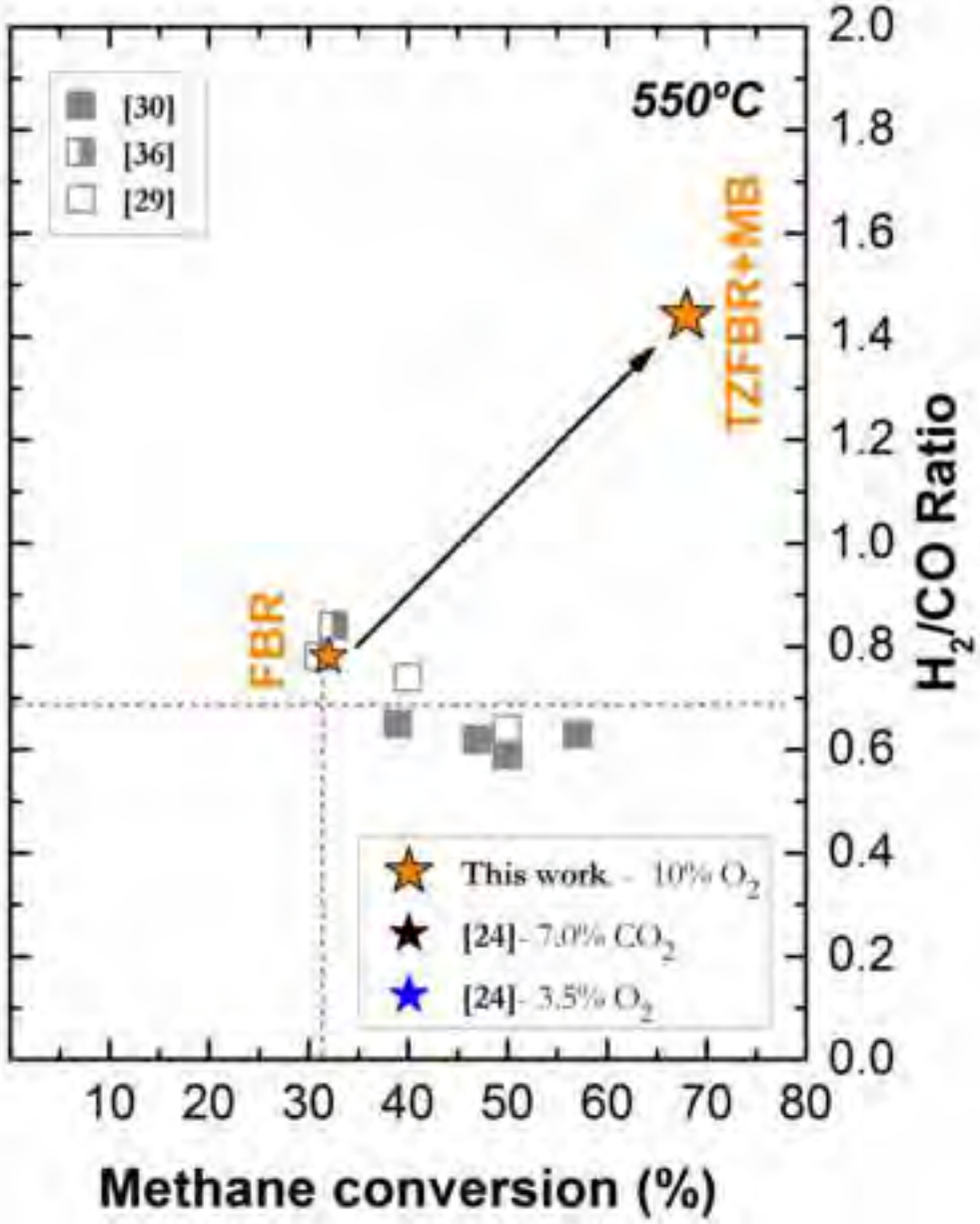

Figure 11 (revised) presentation scheme (pdf format)